



## Neo-Haldanian and bubble models, Bühlmann, bubble grow and Bubble dynamics

Nico A.M. Schellart

### Contents

Summary	1
Ten geleide en verantwoording	2
Samenvatting	2
Neo-Haldanian theory	4
Background and basic concepts	4
Increase and decay of tissue partial N <sub>2</sub> pressure	5
The M-value	10
%M-value	14
The oxygen window	16
Bubble models	19
Bubble formation	19
The Varying Permeability Model	20
New developments	23
References	24
Abbreviations and symbols	25
Appendix 1 A deeper dive into VPM and RGBM	26
Surface tension	26
Gas bubbles in liquid	26
Bubbles and diffusion	27
The surfactant as bubble stabiliser	28
From equilibrium to in- and outflow	29

***Dit document is een vrijwel exacte kopie van een les gegeven door de auteur voor de cursus "Decompressie-recompressie" van de Scott Haldane Foundation, Zwolle, 2 juni 2006.***

***Rapport SR-06-02, mei 2006***

© Copyright Scott Haldane Foundation en Stichting Duik Research, 2006. Beperkte overname is toegestaan mist voor niet-commerciële doeleinden en indien de bron vermeld wordt.

© Copyright Scott Haldane Foundation en Stichting Duik Research, 2006. All rights reserved. Material of this lesson may not be reproduced in any form without permission of SHF and SDR. An exception is made for educational purposes, provided that there is no financial profit.

## Summary

Only one aggregation condition, the liquid phase, is relevant for calculations with Haldanian models. Therefore, these models are also called liquid models. In the liquids, the compartments of the model - in reality the tissues - various gases are dissolved. With the half times ( $T_{\text{half}}$ ) of the compartments, the on-going partial  $N_2$  pressures ( $PN_2$ ) of the compartments are calculated. On the base of a compartment *and* depth dependent criterion, the M-value, it is determined whether ascending to surface or the first stop is allowed with the momentary compartment  $PN_2$ . None of the compartment should exceed the criterion for ascending.

In the Bühlmann model, the M-values can be calculated with **a** and **b** coefficients, which are directly calculated from  $T_{\text{half}}$ . The nature of the Neo-Haldanian models is the compartment specific M-value comprising two coefficients.

The other important aggregation condition, the gas phase, is not implied in the liquid models since it is assumed that all  $N_2$  is dissolved. Free gas, in bubbles, is not present. However, these models explicitly attempt to avoid the formation of bubbles.

The  $N_2$  gradient of off-gassing between tissue and capillaries is maximised by decreasing the ambient  $PN_2$  as much as possible, such that on the one hand off-gassing is as fast as possible and on the other hand the risk on DCS does not increase above a chosen criterion (e.g. 1%). The balance between both is based on empirical data. Actually, the process of off-gassing can only be calculated since the  $pN_2$  of tissues is hardly measurable directly and is therefore seldom done (animal models).

In the first part of this contribution one learns about the fundamentals of the liquid models.

The complex but elegant Fig. 5 summarises the complete Neo-Haldanian theory.

Bubble models, such as VPM (Variable Permeability Model) and RGBM (Reduced Gradient Bubble Model), for which Yount provided the basis, also take the gas phase, so bubbles, into account. The second part will discuss the concepts of the bubble models. In these double-phase models, it is tried to limit the total free gas volume to a chosen minimum and so the amount of (pathological) bubbles. This can be achieved by introducing a particular stop, the deep stop, which is at about half the maximal depth. In this way, the bubble can hardly grow, in contrast to bubbles of a large ascent. With the deep stop, the bubble pressure is within some minutes equal to the  $PN_2$  of the surrounding off-gassing compartment and the bubble will also start with off-gassing. The model prescribes an ascent as high as possible, but without exceeding a total critical bubble volume in order to prevent (subclinical) DCS.

New theoretical developments indicate that M-values behave different with altitude and repetitive diving with non-linear depth dependency. Liquid models don't have these refinements and although their recent changes seems to diminish these drawbacks, the changes seem to be rather arbitrarily. In the manuals of diving computers based on liquid models the changes are said to be empirical.

## Ten geleide en verantwoording

De onderstaande Engelse tekst is hier en daar ontleend aan “An explanation Professor A A Bühlmann’s ZH-L16 Algorithm” van Paul Chapman (200x) dat berust op de 4de editie van Bühlmann’s boek “Tauchmedizin”, 1995. Een ander bron is “The trouble with bubbles” van Richard Heads (200x). Dit laatste, wat ook de basis van de bellenmodellen behandeld, heeft een zuiver conceptuele opzet zonder formules, dat van Chapman (alleen vloeistofmodel) enkele formules. Wat meer rekenwerk is te vinden in het hoofdstuk “Decompression theory - neo-Haldane models” van “DeepOceanDiving’s Diving Science”, van Van de Velde (1999-2005).<sup>1</sup> Deze laatste website heeft ook een hoofdstuk over bellenmodellen maar dat is een nogal mathematische samenvatting van de theoretisch-fysische artikelen over de bellen modellen en niet geschikt voor lezers die in dit soort artikelen niet goed thuis zijn.

Uit genoemde publicaties (en in mindere mate van en paar andere) zijn zinnen en passages van ongewijzigd tot sterk gewijzigd overgenomen, evenals figuren. Daarnaast is een enkel figuur, zij het gemodificeerd, ontleend aan Bühlmann (1989) en Reinders (200x). Het merendeel van de tekst en illustratiemateriaal is evenwel van mijn hand. De cursieve stukjes en de appendix (evenals een aantal voetnoten) gaan wat dieper op de stof in, maar zijn voor het conceptuele begrip niet noodzakelijk. Cursief en tevens onderstreepte tekst bevat een ‘take home message’.

De auteur realiseert zich dat onderstaande schriftelijke les moeilijk zal zijn voor hen die zich niet regelmatig met de fysiologie bezighouden. Ook wordt opgemerkt dat het hier en daar mogelijk kan zijn dat de theorie niet geheel correct is weergegeven. Enerzijds kan dit door de auteur gewenste vereenvoudiging betreffen, maar anderzijds ook een niet geheel juiste interpretatie.

De lezer wordt geadviseerd eerst de decompressietheorie van een boek over de opleiding van de (ver)gevordede (sport)duiker te lezen, bijv. “Opleiding 3\* NOB”, 2004, ISBN 90-71022-08-1. Hierdoor zal de stof van deze bijdrage veel makkelijker begrepen worden.

## Samenvatting

Haldaniaanse modellen rekenen slechts met één aggregatietoestand: de vloeistoffase. Ze zullen daarom gemakshalve de vloeistofmodellen genoemd worden. Hierin zijn de diverse gassen opgelost. Voor de diverse “weefsels”, of beter compartimenten, worden dan op grond van hun halfwaardetijd,  $T_{\text{half}}$ , de bijbehorende  $pN_2$  berekend. Aan de hand van een criterium, de M-waarde, dat zowel van het compartiment als de diepte afhankelijk is, wordt bepaald of met de actuele  $pN_2$  mag worden opgestegen naar de oppervlakte of de geringste stopdiepte. Aan het criterium moet dus gelijktijdig door alle compartimenten voldaan worden. De M-waarden volgen in het model volgens Bühlmann uit zijn **a** and **b** coëfficiënten die steeds met dezelfde formule uit  $T_{\text{half}}$  te berekenen is. De M-waarden met twee coëfficiënten is het kenmerk van de Neo-Haldaniaanse modellen.

De andere essentiële aggregatietoestand, de gasfase wordt niet meegenomen in de berekening, omdat aangenomen wordt dat alle  $N_2$  is opgelost. Gasbellen komen in de compartimenten dus niet voor. Wel beogen al deze modellen uiteraard expliciet de vorming van bellen te voorkomen.

De  $N_2$  uitwasgradiënt tussen het weefsel en arteriën wordt gemaximaliseerd door de  $N_2$ -druk van de omgeving zover mogelijk te verlagen, zodanig dat enerzijds het uitwassen (off-gassing) zo snel mogelijk is en anderzijds de kans van het optreden van DCZ een

---

<sup>1</sup> Overname uit genoemde bronnen is conform de copyrights.

gekozen criterium (bijv. 1%) niet overschrijdt. Dit laatste berust op experimentele data. Het proces van uitwassen kan eigenlijk alleen theoretisch berekend worden. Immers de  $pN_2$  van de weefsels is uiterst lastig op directe wijze te meten en dat wordt zelden gedaan (diermodellen).

In het eerste deel van deze les leert men de grondslag van de vloeistof modellen. De complexe maar elegante Fig. 5 bevat de totale Neo-Haldaniaanse theorie.

Bellenmodellen, zoals de modellen VPM (Variable Permeability Model) en RGBM (Reduced Gradient Bubble Model), waarvoor Yount de grondslag legde, nemen ook de gasfase mee. Het tweede deel van de les zal ingaan op de onderliggende concepten van de belenmodellen. In deze vloeistof-gas modellen wordt getracht het totale gasvolume zo klein mogelijk te houden, zodat er zo min mogelijk belen zijn. Dit kan door de eerste stop, de zgn. diepe stop, voldoende diep te houden, zodanig dat de beldruk net wat lager is dan de druk in het omringende compartiment. Hierdoor kunnen ze nauwelijks of niet groeien en binnen enkele minuten wel gaan krimpen. Er wordt dus zover mogelijk opgestegen, maar zodanig dat de belen een gezamenlijke kritische volume niet overschrijden om (subklinische) DCZ te vermijden.

Uitwerking van deze theorie toonde aan dat de M-waarden zich anders dan die van de Neo-Haldaniaanse modellen gedragen, i.h.b. bij bergmeerduiken en bij herhalingsduiken. Ook is beschreven dat ze niet-lineair diepte afhankelijk kunnen zijn. De vloeistofmodellen kennen deze en vele andere verfijningen niet. Hoewel recente aanpassingen van de vloeistofmodellen deze tekortkomingen verkleinen lijken deze min of meer arbitraire, maar wel empirische aanpassingen.

## Neo-Haldanian theory

### Background and basic concepts

The models are supposed to describe the actual processes in human bodies accurately enough, so that they can be used to plan dives (and other pressure exposures) and in order to avoid decompression sickness (DCS). It is important to realize that the models are arbitrary in the sense that they do not represent the actual physical processes, which are taking place. They simply attempt to model the real-life results mathematically.

The Scottish scientist John Scott Haldane is generally considered the founding father of modern decompression theory. Research on caisson workers suggested that gases, breathed under pressure, were diffusing into the body's tissues and when these gases came out, in the form of bubbles in the body, the workers obtained caisson disease, or what now is called DCS. Haldane's work led him to consider the body as a group of compartments in parallel. So, the compartments were all exposed simultaneously to the breathing gases at ambient pressure, but able to react to them in their own way. No gas transfer from one compartment to another was considered. This principle is still in use and is the basis of many, but not all, current decompression models. The model used for the BSAC-88 dive tables (British Sub Aqua Club) used a single block of "tissue" along which gas diffused. The Canadian DCIEM model uses a range of compartments, but arranged in series - only the first one is exposed to the ambient pressure - and gas transfer by perfusion and diffusion takes place from one compartment to the next.

Surprisingly, none of the current models comprises the blood as first compartment with all the others parallel beyond. This would much better represent the physiology. Since the blood has a halftime ( $T_{\text{half}}$ , see next section) of about 60 seconds (depending on the heart minute volume (HMV), mathematically the difference with the all-parallel models is fortunately small. This series-parallel model although much more complicated is not too hard to model mathematically for the physicists, but much work of calculating<sup>2</sup>.

Haldane also noticed that the body could tolerate a certain amount of excess gas with no apparent ill effects. Caisson workers pressurized at 2 bar (10 meters) experienced no problems, no matter how long they worked. These two ideas, gas diffusing through the body tissues and perfusing through the blood, and the theory of a "tolerable overpressure" formed the basis of Haldane's work. The challenge was to model exactly how the gas moved through the body and exactly what amount of overpressure was acceptable and Haldane actually achieved this with considerable success. Others developed Haldane's ideas over the years. In the sixties USN physician Robert Workman refined the idea of allowable overpressure in compartments, discounting oxygen and considering only inert gases in the breathing mix, such as  $N_2$  and He. Workman's maximum allowable overpressure values, what he called M-values, were more complex than Haldane's, since they vary with depth and with compartment type.

In the classical model of Haldane, it is allowed to ascent to a depth where the maximal allowed compartment inert pressure is twice the ambient inert gas pressure. This factor of 2, the M-value of Haldane, holds for all compartments. So, when for all compartments this factor is less than 2 one is allowed to ascent.

---

<sup>2</sup> The parallel compartments, together forming a multi-output linear system, load the blood (the blood 'sees' the parallel compartments. Physically this means that between the blood compartment and the parallel compartments there is no 'separation of impedance'. The inert gas pressure of the blood can not longer be described by a single halftime. For the calculation of the pressures in the parallel compartments that of the blood is used rather than that of the inspired gas.

Also in the sixties, Professor Albert Bühlmann started to work on similar research at the University Hospital in Zurich. Bühlmann's research spanned over 30 years and was published as a book, *Dekompression – Dekompressionskrankheit* in 1983. This book made fairly comprehensive instructions on how to calculate decompression available to a wide audience for the first time and therefore Bühlmann's work became the basis for many dive tables, dive computers and desktop decompression programs.

If pressure is reduced too much, bubbles will form in the actual tissue (and generally also in the arterial blood), since the gas will be unable to diffuse out of the tissue into the blood and then back via the bloodstream to the lungs.

Before proceeding, first the types of bubbles will be discussed. In the literature four names of bubbles can be found. Unfortunately, often they are not or sloppy defined and sometimes completely wrong (UWATEC manuals implicitly define micobubbles as Doppler detectable, but without DCS symptoms). Here, I will make a distinction between silent and microbubbles. The types are distinguished as follows:

- 'real' bubbles, detectable with Doppler echocardiography or in the pulmonary artery by a skin-Doppler probe placed in the third intercostal space. With the first technique they have diameters generally  $> 20 \mu\text{m}$  and with the latter detected bubbles have diameters  $> 50 \mu\text{m}$ . When such bubbles pass the lung (via anastomoses) or pass an open foramen ovale they can block vessels, so they are pathologic and dangerous. Yet, their effect is often subclinical;
- 'silent' bubbles, 7 to 15  $\mu\text{m}$ , so undetectable by the Doppler technique. They can be pathologic and can block capillaries;
- 'microbubbles', ca. 1.2 to 7  $\mu\text{m}$ , too small to block capillaries. They pass the lung and then they can grow to become a silent bubble;
- 'nuclei' or 'seeds', of the order of some nm to ca. 1.2  $\mu\text{m}$ . They are always present, possibly in huge amounts. Their diameter is often below a critical diameter to grow.

The diameter of 1,2  $\mu\text{m}$  is variable and dependent on many factors (see Bubble Models). Beyond this value bubbles shrink and above this value they grow.

Bubbles and silent bubbles may give rise to the symptoms of DCS. So, how much pressure reduction is too much? It has been shown empirically that faster tissues like blood can tolerate a greater drop in pressure than slower tissues, without pathological bubble formation. One of the historical challenges was to calculate this reduction that could be used to help constructing and planning decompression profiles.

### Increase and decay of tissue partial $\text{N}_2$ pressure

Due to differences in perfusion, diffusion and other factors, the inert gases are dissolved into different body tissues at different speeds. Tissues with high rates of diffusion and a good blood supply, build up a gas load more quickly. The blood itself, major organs, and central nervous system fall under this heading and they are called "fast" tissues. Other tissues build up a gas load more slowly. Progressively slower tissues include muscle, skin, fat and bone. Generally, in the process of gas transport, perfusion dominates diffusion. Tissues with good blood supply are exposed within some minutes to higher inert gas pressures, while others have to wait tens of minutes before gas can reach them by diffusion from other surrounding tissues. Examples are parts of bony and cartilage tissues and the optical eye media which lack vessels. These latter tissues are (at least) the third of the series cascade blood, blood-supplied tissue, not- blood-supplied tissue. So, in reality,

the body tissues are both serial and parallel. It should be clear that such a mixed system is more difficult to model. Even a series-system is not that simple as the parallel system.

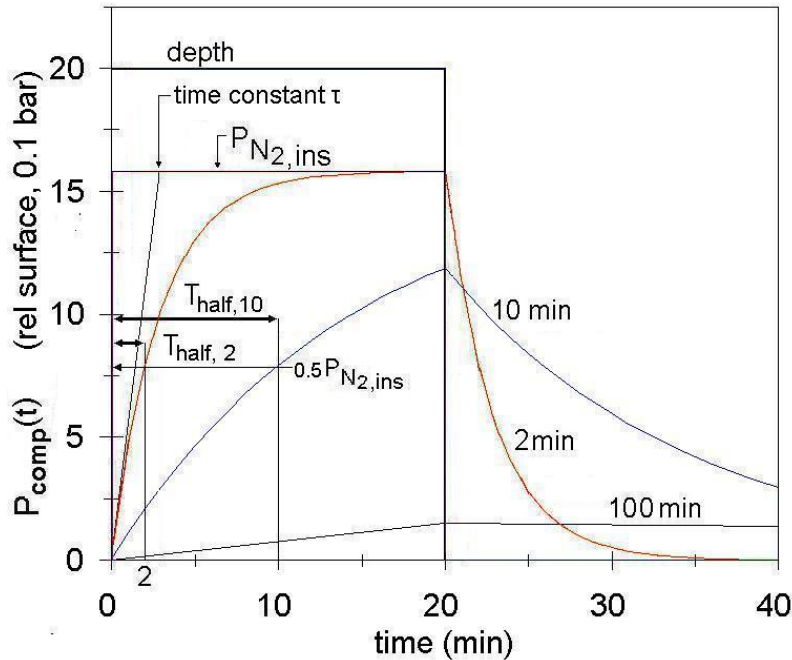


Fig. 1  $N_2$  on- and off-gassing of a theoretical 2-, 10- and 100-min compartment.  $P_{N_2,ins}$ <sup>3</sup> is the partial  $N_2$  pressure of the inspired gas, here air. After 12 min, six half times, the 2-min compartment can be considered as saturated. During the decompression phase, at  $t=22$  min, the 10-min compartment becomes leading and after some 60 min (not depicted), the 100-min compartment takes over. The time constant  $\tau = T_{half} \ln 2$ . Double-headed arrows give the halftimes of the 2 and 10 min compartments.

Although a fast tissue will build up a higher inert gas load (“on-gas”) more quickly when the pressure increases, it will also be able to get rid of that gas load more quickly than a slower tissue when the pressure drops, a process called off-gassing.

It is assumed that tissues on-gas and off-gas according to the theory of halftimes. Many natural phenomena are described this way, including radioactive decay. Such processes are visualized in Fig. 1. After one  $T_{half}$  the pressure of gas in the tissue will be half way the ambient  $N_2$  pressure ( $P_{N_2,ins}$ ) of the gas outside (or better the inert alveolar gas pressure)<sup>4</sup>. After a 2<sup>nd</sup> period of  $T_{half}$ , the gas pressure in the tissue will have risen by half of the remaining difference making it 75% of the way to match the external gas pressure. After  $6T_{half}$ , it's close enough to the asymptote and the tissue is “saturated”. In Fig. 1, this is at 12 min for the 2-min compartment. At this point gas will diffuse in and out at the same rate. So, a stable equilibrium is reached. If the pressure then increases (the diver goes deeper), the tissue will begin to on-gas again. If the pressure reduces, the tissue will off-gas, again following the  $T_{half}$  principle. After  $6T_{half}$ , the tissue will again be equilibrated with its surroundings.

<sup>3</sup> In contrast to the classical convention (partial) pressure is denoted by 'P', not 'p'.

<sup>4</sup> When the ambient and alveolar partial pressures of  $H_2O$  and  $CO_2$  are considered, then  $P_{alveolarN_2} = 0.790(P_{amb} - 0.05)$  (see also Bühlmann 1993). The factor 0.05 is dependent on the respiratory quotient R.

As Fig. 1 shows, after surfacing slow compartments are finally more loaded with gas than faster compartments, since off-gassing goes slower.

As well as differing for each tissue,  $T_{\text{half}}$  will also vary for different gases, since they diffuse at different rates. For real human tissues  $N_2$   $T_{\text{half}}$ 's will vary from one minute (for the blood; dependent on cardiac output) to many hours. Diffusion rates are reciprocally proportional with the square root of the molecular weight. This gives a factor  $1/2.65$ . However,  $T_{\text{half He}} > T_{\text{half He}}/2.65$  since perfusion dominates and this is independent of particle size.

For his ZH-L16A algorithm Bühlmann chose to divide the body into 16 compartments and give them a range of  $T_{\text{half}}$ 's, from 4 (or 5) minutes to several hours, 635 (or 640) minutes. The halftimes are arbitrarily chosen, but such that they increase with about the same factor. This holds for all neo-Haldanian models. Bühlmann named his algorithm from Zurich (ZH), limits (L), 16 the number of M-values and A the original version. Notice that these compartments are not representing real tissues in the body and the  $T_{\text{half}}$ 's are such chosen to give a representative spread of likely values.

When exposed to pressure, at any time the inert gas pressure in each compartment during on-gassing or off-gassing can be calculated according to its given  $T_{\text{half}}$ . The basic formula is:

$$P_{\text{comp},i}(t) = P_{\text{comp},i,\text{begin}} + [P_{\text{igas},\text{ins}} - P_{\text{comp},i,\text{begin}}] \times [1 - 2^{-t/T_{\text{half}}}] \quad \text{with} \quad (1)$$

$P_{\text{comp},i,\text{begin}}$  inert gas pressure in the compartment at the begin of exposure (bar)  
 $P_{\text{comp},i}(t)$  inert gas pressure in the compartment as a function of the exposure time  $t$  (bar)  
 $P_{\text{igas},\text{ins}}$  inert gas pressure in the mixture being inspired (bar)  
 $t$  length of the exposure time (min)  
 $T_{\text{half}}$  half time of the compartment (min)

Notice that all these pressures  $P$  respect the inert gas, in practice  $N_2$  when breathing air. Equation (1) is the formula describing the on-gassing as illustrated in Fig. 1. These curves are exponential curves, as also holds for the curves indicating the off-gassing. Resuming: on- and off-gassing follows an exponential time course.

The expression  $(1-2^{-t/T_{\text{half}}})$  actually comes from an e-power where  $T_{\text{half}}$  replaces the so-called time constant  $\tau$ . So, the expression is originally  $(1 - e^{-t/\tau})$ . From the physical point of view, it represents the output of a so-called linear first order low pass system with as input a step function (here from surface with  $P_{\text{igas},\text{ins},\text{surface}} = P_{\text{comp},i,\text{begin}} = 0.79$  bar to depth with  $P_{\text{igas},\text{ins}}$ ) and as output  $P_{\text{comp},i}(t)$  to be calculated at any time  $t$ . Such a system cannot follow fast changes of the input. With the step function as input, it starts to integrate the input, but after some time this integrating action fails as shown in Fig. 1 for the 2 and 10-min compartments at the time scale used. The output increases less fast as can be seen in particular for the 2-min compartment (Fig. 1). Therefore this system is also called a leaky integrator: the input leaks away when the asymptote  $P_{\text{igas},\text{ins}}$  at  $t \rightarrow \text{infinite}$  is (nearly) reached. Substituting infinite for  $t$  in (1) directly yields that  $P_{\text{comp},i}(\text{infinite}) = P_{\text{igas},\text{ins}}$  (since  $2^{-\text{infinite}/T_{\text{half}}} = 0$ ). This behavior is most elementary in many biological processes. Examples are the clearance by the kidneys, the decay of many substances in the blood, blood pressure in the proximal aorta, and also the time course of many chemical and physical processes (radioactive decay, the change of temperature of a fever thermometer). The

elegance of an e-power is that the directional coefficient at  $t=0+$  crosses the asymptote exactly at  $t=\tau$  (see Fig. 1).

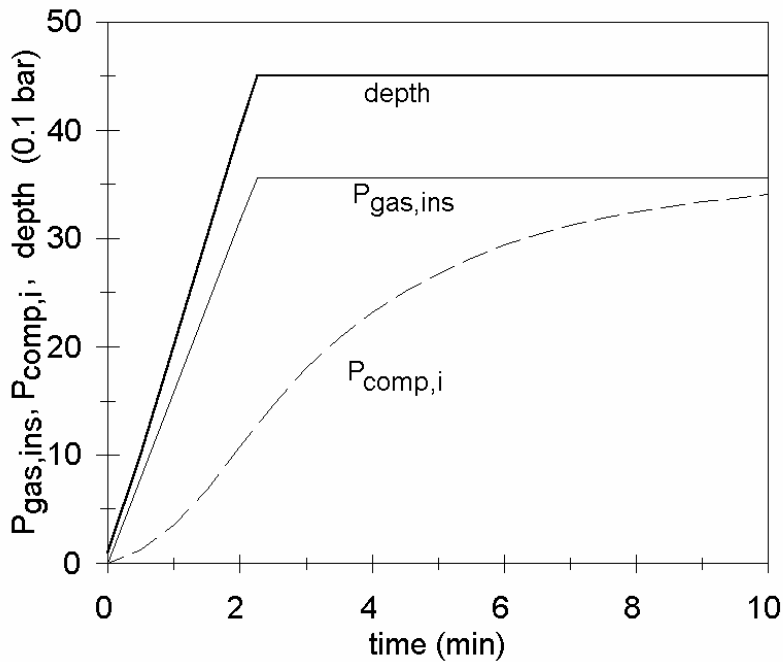


Fig. 2 Effect of a finite velocity of descent on  $P_{comp,i}(t)$ . The same shape of the curve is obtained when a step is applied to a series system, e.g. some tissue in series with the blood. When such a system also obtains a finite velocity as input, the output, ( $P_{comp}(t)$ ) of the tissue starts even more slowly (time derivative is zero at  $t=0$ ).

As a numerical example of the application of (1), a diver is supposed to descend from the surface to 30 meters on air and waits there for ten minutes.  $P_{igas,ins}$  is  $4 \times 0.79 = 3.16$  bar.  $T_{half}$  for example of compartment 5 in ZH-L16 is 27 minutes. The  $P_{comp,i,begin}$  is 0.79, assuming the diver has not already been diving or subject to any altitude changes. The length of the exposure ( $t$ ) is 10 minutes. Using these values in (1), the result is:

$$P_{comp,i,10} = 0.79 + [3.16 - 0.79] \times [1 - 2^{-10/27}] = 1.33 \quad (\text{bar}) \quad (2)$$

In reality, the diver could not have made an instantaneous descent to 30 meters and would have accumulated gas during the descent as well. Averaging the pressure during the descent and repeating the above calculation gives an idea of the uptake during the descent.  $P_{comp,i}(t)$  can be approximated more precisely by repeating the calculation many times with small pressure steps at short intervals during the descent.

*The equation which exactly describes  $P_{comp,i}(t)$  of this descent also comprises a linear term in  $t$ . This results in a less abrupt start of the increase of  $P_{comp,i}(t)$  as shown in Fig. 2. When  $t$  becomes larger the difference with the curve in Fig. 1 is neglectable.  $P_{comp,i}(t)$  at the instant of the arrival at the depth of 30 m should be used as the starting point for the next calculation with (1), the stay at 30 m. Such a stepwise approach of a profile with the slopes of the descents and various ascents to and from various plateau's is a little unpractical.*

*A very flexible approach, which can be used for any profile, no matter how complex, is the application of a convolution integral<sup>5</sup>. I used its numerical equivalent to illustrate my contributions of this and other lessons. The beauty of the convolution integral is its versatility. So, the diver can ascend or descend to/from any pressure, breathe any gas, change gases, go flying after diving, stay on the surface, do a repetitive dive or anything, the convolution integral gives the answer. The calculation can be done real time as in dive computers (DCs). In the lesson 'Duikcomputers en vergelijking duikprofielen' this will be explained a little more.*

After performing the calculations of on-gassing for all the other compartments  $P_{comp,i}(t)$  is known in any given compartment at any time. Next,  $P_{amb,tol}$  is needed so that the depth of a safe ascent is known for each compartment. Bühlmann concluded from a large number of experiments that for each compartment the smallest tolerable ambient pressure that result in DCS for a chosen very small percentage of the dives,  $P_{amb,tol}$  appeared mathematically related to its half-time  $T_{half}$ , as shown before by other investigators. Faster compartments appear to tolerate a greater pressure drop than slower ones. Bühlmann found that  $P_{amb,tol}$  was comprised of two coefficients which he called **a** and **b**.

Each compartment has its own **a** and **b**. They are related to  $T_{half}$ :

$$\mathbf{a} = 2T_{half}^{-1/3} \quad (3a)$$

$$\mathbf{b} = 1.005 - T_{half}^{-1/2} \quad (3b)$$

The resulting 16 **a** and **b** coefficients are the basic parameters of Bühlmann 's ZH-L16A model.  $P_{amb,tol}$  can now be calculated for any chosen  $P_{comp,i}$  at time  $t$  and equals:

$$P_{amb,tol} = (P_{comp,i} - \mathbf{a})\mathbf{b} \quad (4a)$$

*The equation is not dependent on the actual depth and it is irrelevant how  $P_{comp,i}$  is obtained.*

Fig. 3 depicts the linear relationship between  $P_{amb,tol}$  and  $P_{comp,i}$ . When the stop-depth  $P_{stop}$  is chosen,  $P_{stop}$  replaces  $P_{amb,tol}$  in (4a). Then, the maximal  $P_{comp,i}$ , denoted as  $P_{compmax,i}$  is:

<sup>5</sup> *In this case the convolution integral, is:*

$$P_{comp,i}(t) = \int_0^{+\infty} h(\tau) \cdot P_{ig,ins}(t-\tau) d\tau$$

*Now,  $P_{ig,ins}$  is not any longer a constant but a function of time  $t$ . It is  $k$  times the dive profile (in bar) with  $k=0.79$  with air as breathing gas.  $h(\tau)$  is called the unit impulse response of the compartment, which behaves as a low pass first order linear system. For such a system the impulse response is the e-power  $\tau^{-1} e^{-t/\tau}$ . The linear impulse response is the backbone of system theory. It can be found by the inverse Laplace transform of the transfer characteristic  $H(s)$  of the system. To calculate  $P_{comp,i}(t)$  of e.g. multilevel profiles these transform of  $H(s)$  are not practical. More adequate and a good alternative of the convolution integral is using Fourier transforms:*

$$P_{comp,i}(t) = \mathcal{F}^{-1}\{\mathcal{F}\{P_{ig,ins}\} \cdot \mathcal{F}\{h(\tau)\}\},$$

*provided that the dive profile and  $h(\tau)$  are well sampled (in accordance with Nyquist's theorem).*

$$P_{\text{compmax},i} = a + P_{\text{stop}} / b, \quad (4b)$$

where  $P_{\text{stop}}$  and  $a$  are in bar absolute, and  $b$  is dimensionless.

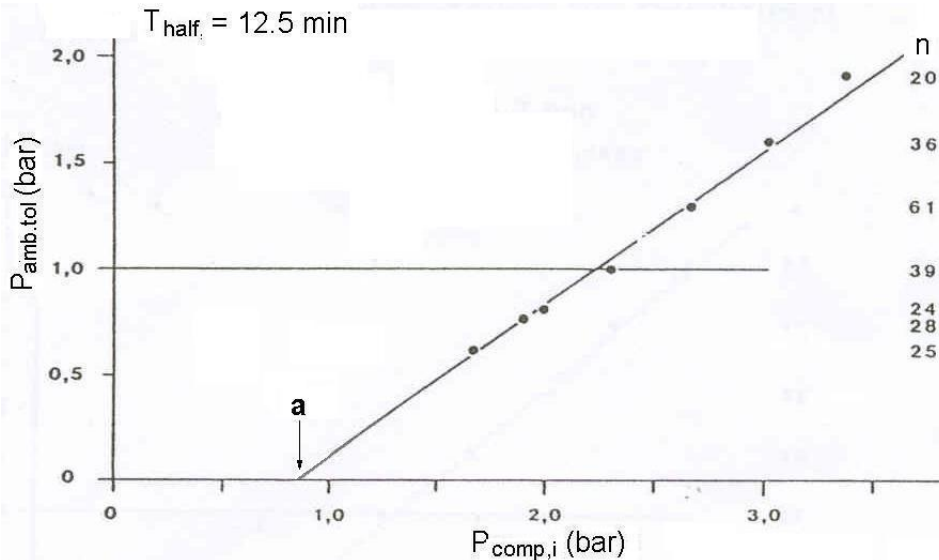


Fig. 3  $T_{\text{half}} = 12.5$  min. The experimental values correspond with the theoretical line according the coefficients  $a$  and  $b$  derived from  $T_{\text{half}} = 12.5$  min. The line is  $P_{\text{amb,tol}} = (P_{\text{comp},i}(t) - 0.86)0.72$ .  $n$  is number of subjects. The points at  $P_{\text{amb,tol}} \geq 1.0$  bar during decompression are determined by simulated dives in a compression chamber. The values at  $P_{\text{amb,tol}} \leq 1.0$  bar are derived from dives in mountain lakes.  $a$  equals the intersection with the horizontal axis and  $b$  the slope of the line. (After Bühlmann, 1989.)

The classical Haldane model has no  $a$  (i.e.  $a=0$ ) and  $b$  is 0.5 for each compartment. For all, except the fastest compartment, this classical model is not enough conservative. The models of Workman en Bühlmann are called Neo-Haldanian due to comprising a  $b$  and an  $a$  coefficient, and moreover, both are different for all compartments.

### The M-value

Many authors use other symbols to indicate Bühlmann's  $a$  and  $b$  in liquid (Neo-Haldanian) models. The generally used M-value/ $\Delta M/M_0$  notation is:

$$10P_{\text{compmax},i} = \text{M-value} = M_0 + d\Delta M \quad (\text{pressure in msw absolute}) \quad (4c)$$

where  $P_{\text{compmax},i}$  is in bar absolute,  $d$  is the stop depth, equal to  $10(P_{\text{amb}}-1)$  in msw (but otherwise with other coefficients in all equations in feet) relative to sea level.

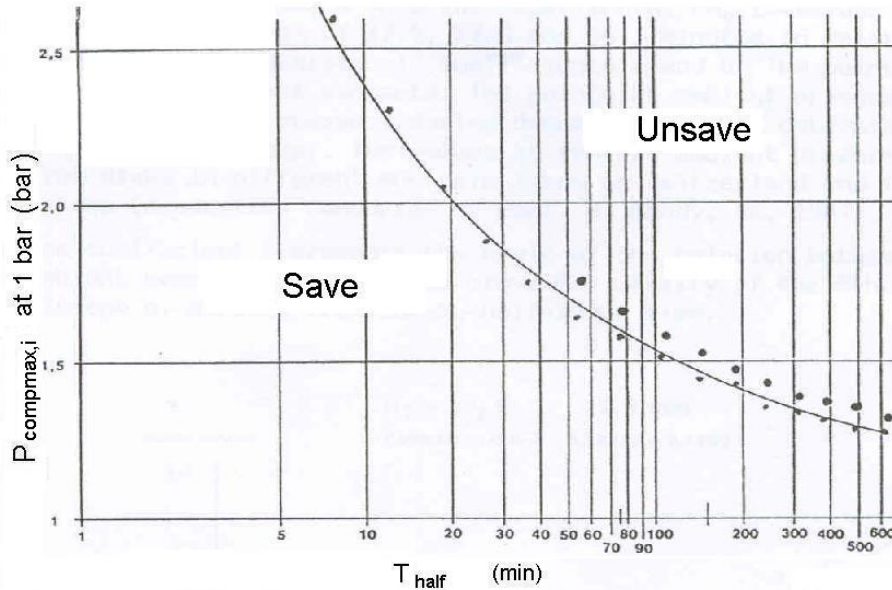


Fig. 4 The  $P_{N_2, \text{tol}}$  (the  $P_{\text{compmax}, i}$  with air breathing) of 15 compartments versus  $T_{\text{half}}$  for air breathing from 8 minutes up to 635 minutes at an ambient pressure of 1.0 bar (surface). The curve is calculated with  $P_{\text{compmax}, i} = a + 1/b$ , see (2b). • Experimental values of 234 subjects with 1.7% slight symptoms of DCS, skin or joints (no repeated dives). ● Experimental values of 80 subjects with insufficient decompression. 42.5% (n=80) symptoms of DCS, skin, muscles, joints (no repeated dives). Notice that an increase of  $P_{\text{compmax}, i}$  of some 0.1 bar results in a risk increase of a factor of 25. The experimental  $P_{\text{compmax}, i}(t)$  was calculated from the dive profile, which was basically performed with the Bühlmann tables. (After Bühlmann, 1989.)

The M-value coefficients are as follows related to the  $a$  and  $b$ :

$$\begin{aligned} \Delta M &= 1/b && \text{(dimensionless)} \\ M_0 &= 10(a+1/b) && \text{(pressure in msw absolute)} \end{aligned}$$

In the Workman Workman/Hempleman notation is  $M$ :

$$M = d\bar{a} + M_0 \quad (4d)$$

So, here  $\bar{a} = \Delta M$ .

Unfortunately there are some flaws in the literature about these coefficients and their definitions (see Wienke 2003, p. 34-35; van der Velde 2002).

After having defined  $a$  and  $b$ , Bühlmann (1989) performed a new series of experiments (544 dives) and analyzed retrospective 573 dives as ultimate test of his coefficients. Most of the dives have been no-decompression dives, using an ascent rate of 10 m/min. The dives had a large range of  $P_{\text{comp}, i}$  obtained with dives to various depths to examine whether the  $P_{\text{amb}, \text{tol}}$  could be predicted from  $a$  and  $b$ . Fig. 3 shows the results for the compartment with  $T_{\text{half}} = 12.5$ .

Of course, (3a) and (3b) are the result of curve fitting. Later, it appeared that especially coefficient **a** needed small upward correction (more conservative) for some moderately fast compartment.

Performing the calculations for all compartments, and taking surface (= 1 bar) as the allowed 'stop-depth', the simple relation between the experimentally found  $P_{compmax,i}$  (notice not  $P_{amb.tol}$ ) - these are the small dots Fig. 4 - and the  $T_{half}$ 's is  $P_{compmax,i} = 2T_{half}^{-1/3} + 1/(1.005 - T_{half}^{-1/2})$ . This can directly be found from (4b) with  $P_{stop}$  is 1 bar (absolute) when (3a) and (3b) is substituted in (4b).

Using the example of equation (1a), it was found that an exposure for 10 min to 4 bar (30 meters depth) led to a  $pN_2$  of 1.33 bar in compartment 5 and the **a** and **b** coefficients for compartment 5 were 0.67 and 0.81 respectively. Applied to (4a) they give:

$$P_{amb.tol} = (1.33 - 0.67) \times 0.81 = 0.54 \text{ bar}$$

The above equation shows that actually ascend to a pressure lower than sea level (i.e. above the surface) is possible. In other word's, according to the model, after 10 minutes at 30 meters (4 bar) the diver could ascend straight to the surface with no bubble formation in compartment 5 assuming air breathing. This is a "no-stop" dive, as expected from looking at dive tables.

Taking a 30-meter exposure for 50 minutes,  $PN_2$  in compartment 5 is 2.5 bar (eq. 1). Then,  $P_{amb.tol}$  is 1.49 bar. This pressure is just shallower than 5 m depth, so this is the maximum depth that compartment 5 would allow us to ascend to after 50 minutes at 30 meters. Using the same depth and time, and repeating this method for all the other compartments, we'll find different values, for example:

Compartment 3 - Half-time 12.5 minutes,  $a = 0.8618$ ,  $b = 0.72$

$$P_{comp,i}(t) = 3.01 \text{ bar}$$

$$P_{amb.tol} = (3.01 - 0.86) \times 0.72 = 1.55 \text{ bar (or 5.5 meters depth)}$$

Compartment 11 - Half-time 187 minutes,  $a = 0.35$ ,  $b = 0.93$

$$P_{comp,i}(t) = 1.18 \text{ bar}$$

$$P_{amb.tol} = (1.18 - 0.35) \times 0.93 = 0.77 \text{ bar (far above the surface, about 2.2 km altitude)}$$

Once this is repeated for each compartment, the diver cannot ascend any shallower than the deepest of the tolerated depths. In the above three-compartment example, this is 5.5 meters. This is called the "decompression ceiling" and the compartment concerned (compartment 3) is said to "control" or lead the decompression at this time. *In general, faster compartments will control short, shallow dives. Long shallow dives and short, deep dives will show a shift towards the middle compartments as controllers. Long deep dives will be controlled by the slower compartments* (see for an example Fig. 6). *The controlling compartment will often shift during decompression.* For example, a short deep exposure may show the initial ceiling limited by the fastest compartment, but as these off-gas quickly the control shifts generally to the 2<sup>nd</sup> compartment and so on, up to the slower, mid-range, compartments.

*Planning a decompression for the 30 meter, 50 minute dive, allows an ascent right up to the 5.5 meter ceiling. However, it is more usual to choose nearest multiple of 3 m that is deeper than the decompression ceiling, so here 6 m. At this point  $P_{comp,i}$  in the more highly loaded compartments will be above the  $P_{igas,ins}$  in the breathing gas and those compartments will start to off-gas. Other compartments may have a  $P_{comp,i}$  lower than*

$P_{\text{igas,ins}}$  and these compartments are on-gassing. At 6 m the  $PN_2$  in air is  $1.6 \times 0.79 = 1.26$  bar. In the example, the  $N_2$  pressure in compartments 3 and 5 was 3.01 bar and 1.33 bar respectively. These are both higher than the 1.26 bar ambient  $PN_2$ , so compartments 3 and 5 will off-gas at this decompression stop. The  $PN_2$  in compartment 11 however has only reached 1.18 bar. The 11th compartment will continue to on-gas at 6 m, although 5 times slower than before because the difference between  $P_{\text{igas,ins}}$  and  $P_{\text{comp,i}}(t)$  is about 5 times lower than at 30 meters. The ceiling will gradually get shallower as the compartment off-gas, eventually reaching next stop depth (3 meters) chosen. At this point the diver ascends to this depth and starts the process again, until he reaches a point where for all compartments  $P_{\text{amb,tol}} \leq 1$  bar and he can reach the surface.

For ascending to shallowest possible standard stop-depth, a multiple of 3 m, for each of the compartment should hold that  $P_{\text{amb,tol}} \leq P_{\text{minimal stopdepth}}$ . Consequently the highest found  $P_{\text{amb,tol}}$  has to be rounded upward to the first multiple of 3 m (or 10 ft), surface and hypobaric conditions (altitude, aviation, space excursions) included.

Calculations have to continue at the surface since compartments continue to off-gas. In this way, the actual loading of the compartments can be used in the calculation of  $P_{\text{comp,i}}(t)$  of the next dive. So, at the start of the next dive the constant 0.79 in (1) is replaced by  $P_{\text{comp,i, end surface interval}}$ .

Bühlmann made several modifications to his original algorithms. For dive table production, the **a** coefficients were altered to be a little more conservative, principally in the middle compartments, resulting in a variation of the algorithm called ZH-L16B. Further variations to both middle and upper **a** coefficients are used in ZH-L16C, intended for use in dive computers, where the exact depth and time tracking removed some of the natural conservatism associated with table use.

Modifications include planning dives deeper and/or longer than actual, further tweaking of the **a** and **b** coefficients to limit the M-values, limiting  $P_{\text{amb,tol}}$  of the compartments to a percentage of the calculated value, changing the amount of inert gas, using longer half-times for the off-gassing phase of the profile, adding more compartments and any number of other factors and combining such modifications. Dive computers and planning programs for PCs, typically implement these modifications and/or variations of their own in an attempt to make the dive profiles they generate more realistic, or more usually, just "more conservative". Attempts to include the effects of factors enhancing DCS risk led to the ZH-L8 ADT "adaptive" algorithm, implemented on the Aladdin dive computers produced in the mid-nineties and later. Recently, for the Smart UWATEC, the coefficients have been made again more conservative, this time substantially.

The discussed formulas use basically inert gas partial pressure throughout, so diving with Nitrox is also accommodated. Likewise Trimix ( $O_2$ ,  $N_2$  and He mixes) and alternative decompression-gases (usually with lower proportions of inert gas) can all be accommodated within the same basic algorithm as long as the half times and the **a** and **b** coefficients (or  $M_0$  and  $d\Delta M$ ) are known for the gases. Where multiple inert gases are used, an intermediate set of **a** and **b** coefficients are calculated based on the gas proportions.

He is a more deco-friendly gas than  $N_2$ . As well as the benefits of narcosis reduction, decompressions are faster and are highly efficient in bottom mixes and I surmise also during decompression, especially when oxygen cannot be used due to depth (intoxication limit). He is expensive and for sport diving only feasible when rebreathers are used.

Unfortunately, these are still expensive. Their use should be simple enough, economically and safely for the average scuba diver to take advantage of mixtures.

The %M-value

Fig. 5 summarizes the M-value concept. The M-value is the theoretical threshold gas load in a compartment beyond which a high frequency of symptoms of DCS can be expected in the majority of divers. Along the vertical axis  $P_{comp,i}(t)$  and along the horizontal axis the ambient pressure are given, both absolute and in bar. In case of air breathing the 'Line of inert gas saturation' has a slope of 0.79. The M-Value Line holds for compartment no.  $n$ . It has a slope of  $1/b$  for 1 bar (0 m) and intersection with the vertical axis at  $a$ . For this compartment the momentary inert gas pressure  $P_{comp,i,n}(t)$  is not allowed to exceed the M-Value Line at any moment on the risk of DCS. Therefore, the area above this line is called the Forbidden Zone. For a dive at sea level,  $P_{comp,i,n}(t)$  can never exceed the M-Value Line. The area between the Line of inert gas saturation and the M-Value Line is the Decompression stop Zone, where stops are obligate. For sea level-dives and altitude dives the area below the safety line and the dashed part of the Line of inert gas saturation is safe. Therefore, it is called the Zone of no-stop dives.

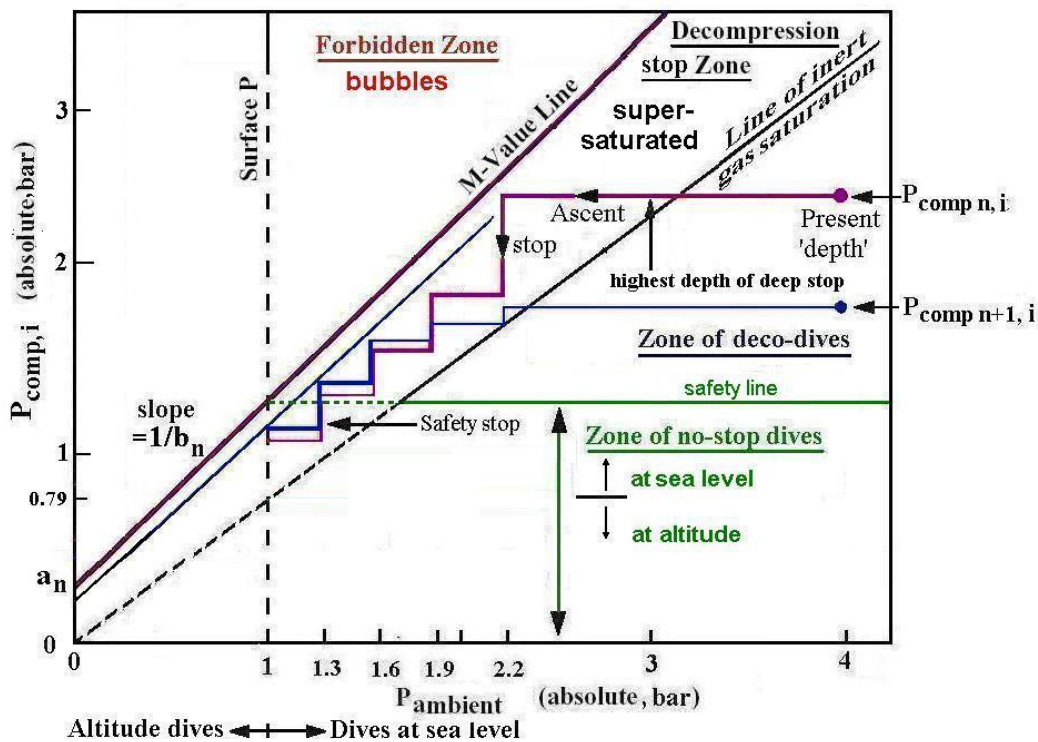


Fig. 5 The M-value concept The thin oblique line below the fat oblique line (M-Value Line) is the M-value line of compartment  $n+1$ . The stair case-like thick line, presenting the ascent profile starting at 4 bar and is indicated by  $P_{comp n,i}$ . Note the large overpressure gradient generated during the ascent to the first stop at 12 m. It is out of proportion to the rest of the deco-profile. The largest depth of a deep stop is at 20 msw (3 bar). The stair case-like thin line, presenting the ascent profile, starts also (of course) at 4 bar and is indicated by  $P_{comp n+1,i}$ . (The original basis of this figure comes from Baker, see Heads, 200x.)

Theoretically even the safety stop can be missed. Notice that the Forbidden Zone and the Decompression stop Zone is dependent on the compartment due to the M-Value Line dependency on the half time.

It is emphasized that the M-value line is actually a gray zone. Approaching the line from below does rapidly increase the risk of bubble formation and grow.

It is supposed that at the start of the ascent compartment  $n$  is leading (often this will be the first compartment). The course of  $P_{\text{comp},n,i}$  is indicated by the fat purple line. Horizontal left movements along the line are ascents (for simplicity infinite fast and therefore  $P_{\text{comp},n,i}$  is constant) and downward movements stops which lasts several minutes. After the ascent to 6 m the compartment  $n+1$  becomes leading since its load has practically reached its M-value line (oblique thin line below the thick M-value line of compartment  $n$ ) and therefore compartment  $n+1$  is more on risk.

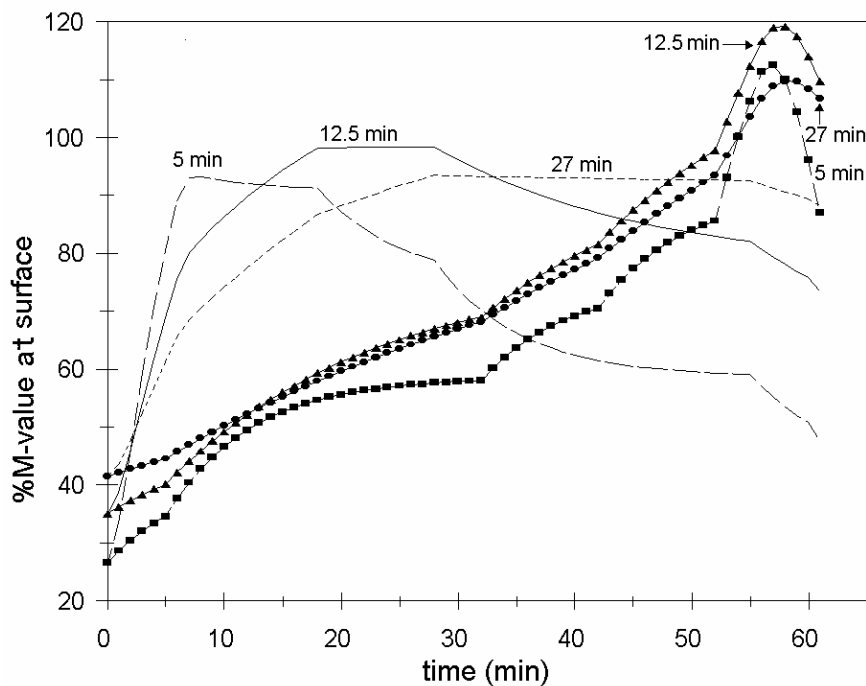


Fig. 6 Reverse profile The %M-value calculated for a direct ascent to 0 m (surface) of the 5, 12,5 and 27 min Bühlmann compartment, calculated for two multilevel profiles being in time each other mirror image. The regular order of the levels is: 6 min (level time) at 45 m, 12 min at 24 m, 10 min at 18 m, 27 min at 12 m and 5 min at 6 m, with the descent included in the 45 m level and ascent time included in the level to be reached. The %M-values of the reversed profile are depicted with symbols. They rise to values that make stops necessary. Those of the regular, correct profile are depicted with drawn and dashed lines without symbols.

Various factors, like heat, cold and exertion change half times and therefore influence  $P_{\text{comp},i}$  and so the profile of the ascent. Increasing  $T_{\text{half}}$  is always a drawback for the deco-phase since one will end up with a higher  $P_{\text{comp},i}$ . This leads to the rule: higher half times lengthen deco-times and no-fly times. Prevent factors which lengthen half times. This holds during the whole dive and especially during the ascent.

All kind of factors respecting the profile, diving history (repetitive diving etc., DCS history), the environmental diving condition, personal characteristics such as the susceptibility to nuclei formation and growing of bubbles etc. affect the risk on pathological bubbles (silent and Doppler-detectable). However, only some factors are used in the liquid models or modified versions. A huge number of factors affect inert gas absorption and elimination, and so DCS risk. Some are implemented in or affect the liquid-models, some cannot be implemented easily and sufficiently on a physical basis (such as repetitive diving, multiday-diving). Some could only be implemented physically into the two-phase models. For these factors the liquid models are in some way 'repaired' but the theoretical basis and the way how is enigmatic. Whether or not an aggravating factor is implemented in a model or dive computer, always take it into account.

To express the extend of  $P_{\text{comp},i}$  in relation to the M-value a new variable has been introduced, %M-value, defined as:

$$\underline{\%M\text{-value} = 100P_{\text{comp},i}(t)/M\text{-value. (in \%)} \quad (5)}$$

Its practical use is that the  $P_{\text{comp},i}$  of various compartments in relation to their M-value can be compared. The compartment with the highest %M-value is most critical, since its risk on bubbles is highest. Its use is illustrated with the example below.

Heavy workloads, reverse profiles and cold enhance bubble formation. The Neo-Haldanian theory explains the ratio of these 'rules' and empirical facts and get rid of them<sup>6</sup>. Here, an explanation will be restricted to the reverse profile, which %M-values are depicted in Fig. 6. The fast compartments clearly succeed in following  $P_{\text{igas},\text{ins}}$ . So, close to the end of the reversed dive when the descent to, here, 45 m is made, the fast compartments are already rather well loaded. At the end of the 45 level the %M-values are much larger than with the normal profile (Fig. 6). The figure clearly shows that a reverse profile produces much higher %M-values and should therefore be avoided.

### The oxygen window

At sea level with breathing air, the arterio-venous (a-v) difference of the blood  $O_2$  content,  $C_{O_{2a-v}}$  is about 4.5 mL/100mL blood.  $PCO_2$  increases only 0.007 bar (5 mmHg) from the arterial to venous blood but the a-v  $PO_2$  difference,  $PO_{2av}$  is some 0.067 bar (51 mm Hg). So, the  $PCO_2$  does not compensate the deficit. The arterio-venous absolute pressure deficit is called the oxygen window. Fig. 7 illustrates how the  $PO_2$  is decreasing along the pathway air→alveoli→arterial blood→venous blood→tissues. Fig. 7 summarizes the partial pressures of the other gases in the compartments from the outside air (air breathing) to the  $O_2$ -consuming tissues. When comparing the partial gas pressures of the arterial blood with the inspired air there appears to be already an arterial window, be it small:  $PO_{2a} < PO_{2alv} < PO_{2ins}$  (subscript a is arterial). At the other side of the  $O_2$  transport line, in the tissues,  $PO_{2tis} < P_{O_{2v}}$  (subscript v is venous).

When  $PO_{2a}$  increases, the blood  $O_2$  content  $C_{O_2}$  also increases, in accordance with the  $O_2$ -dissociation curve. When moving over this S-shaped curve to its nearly horizontal part at the right by increasing  $PO_{2a}$ , caused by increasing the ambient pressure or by breathing e.g. oxygen, the  $P_{O_{2a-v}}$  is increased very substantially since  $C_{O_{2a}}$  and  $C_{O_{2v}}$  shift upward,

<sup>6</sup> The liquid models implement the effects of these factors, but not always enough, in contrast to the bubble models.

and due to the rather pressure independent metabolic utilization of  $O_2$  in the tissues the  $C_{O_{2a-v}}$  is practically constant. Therefore the  $CO_2$  production is constant and  $PCO_{2v}$  is also constant. (Actually a high  $PO_{2a}$  causes hypercapnia, see Schellart, 2002.)  $PCO_2$  increases much less than the decrease in  $PO_2$  due to two reasons. First, not all  $O_2$  consumed is converted to  $CO_2$ . Under normal conditions, only ca. 80% of  $O_2$  is converted to  $CO_2$ . The second and more important reason is that  $CO_2$  is 20 times more soluble in blood than  $O_2$ . Gases that are more soluble produce a lower partial pressure when a given volume of gas is absorbed into a liquid. So,  $C_{O_{2a-v}}$  is rather constant whereas  $P_{O_{2a-v}}$  increases very substantially, and consequently the oxygen window increases.

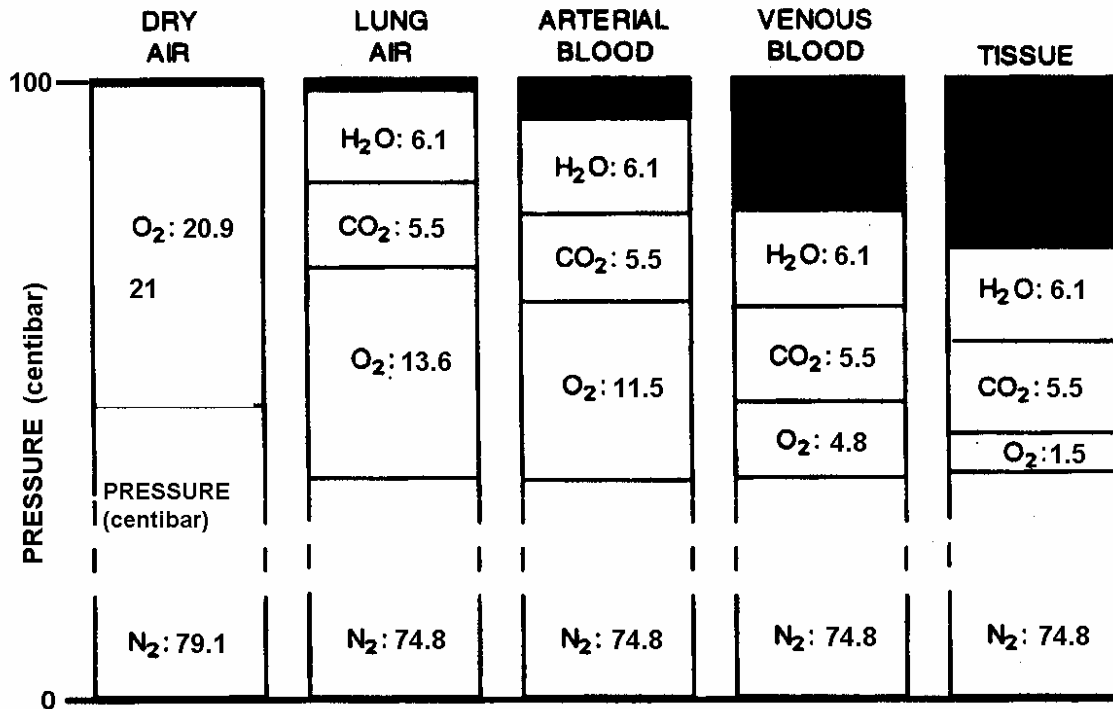


Fig. 7 The partial pressures in dry air, the lungs, and as dissolved gases, in arterial en venous blood and a tissue at an ambient pressure of 1 bar (surface). The black part is the oxygen window. All pressures in centibar (with dry air also in volume%). (Modified after Wienke, 2003.)

When the  $PO_{2,ins}$  is increased above at a certain point the venous Hb is also completely saturated with  $O_2$ . The delivery of  $O_2$  in the tissues is solely provided by the dissolved  $O_2$ . From this point the  $Co_{2a-v}$  becomes constant, as illustrated in Fig. 8. The oxygen window in the venous blood can be occupied by any non-respiratory gas, e.g. by nitrogen provided by the tissues. This happens when during the ascent air breathing is replaced by oxygen breathing. Then, part of the (enlarged) window is filled by nitrogen. Oxygen or oxygen enriched air breathed during a (deep) stop shallower than 15 m after a deep deco-bounce dive is a perfect and save way to shorten total surface time.

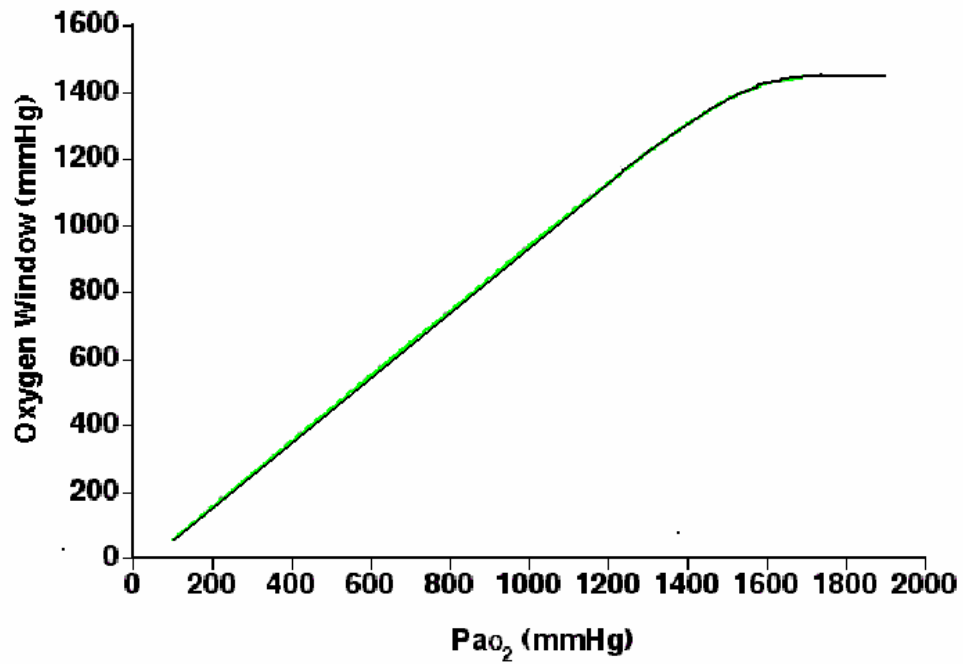


Fig. 8 The oxygen window in the venous blood as function of  $PO_{2a}$ . (Heads, 200x.)

## Bubble models

Although the basic mathematics of bubble models is not very difficult, the mathematics is of quite another caliber than that of the liquid models. Extensive bubble models comprises some 100 parameters and some hundred equations, although many multiple (as much as compartments) and so the physics is complex. I will try to discuss the fundamental concepts and explain the most basic equations.

From Doppler studies, it is known that bubbles are generated after most dives. Although causing no noticeable symptoms, gas elimination from these bubbles and bubbles undetectable by the Doppler technique (the silent bubbles) occurs differently from gas dissolved in the blood. A reduction in ambient pressure will cause these bubbles to grow. Bühlmann's algorithm assumes that all gas, dissolved with supersaturation, is being eliminated in the dissolved phase (i.e. dissolved in the compartments). So, this algorithm does not take free gas into account, in contrast to the bubble models as VPM (Variable Permeability Model) and RGBM (Reduced Gradient Bubble Model). These models describe the interactions between bubbles and liquid, and especially focus to physical and physico-chemical phenomena at the interface between the bubble and liquid (i.e. the tissue).

Doppler monitoring has revealed the presence of bubbles in divers ascending even from relatively shallow dives. These bubbles can result in symptoms such as headache and fatigue in the immediate post-dive phase. These symptoms were considered as subclinical but nowadays these bubbles are thought to cause some damage. Although there is a great deal of plasticity within the human systems and much damage maybe reversible, research suggests that some cumulative injury results in permanent damage. And this occurs without overt symptoms of DCS.

The amount of pathological bubbles (detectable and silent) progressively increases with multi-day repetitive diving. Large prospective trials are needed to properly ascertain whether permanent damage is rigorously and statistically associated with especially deep, repetitive diving and microbubble formation.

### Bubble Formation

The development and evolution of gas phases and bubble formation involves a number of overlapping steps. These include nucleation and their stabilization, supersaturation (dissolved gas build-up), excitation and growth (free dissolved phase interaction), coalescence (bubble aggregation) and deformation and occlusion (tissue damage and ischaemia). Where bubbles form or lodge, how they migrate, how they evolve and dissolve as well as the complete spectrum of physico-chemical insults that results in DCS are not known in great detail. Bubbles may form *de novo* at supersaturated sites on decompression or may grow from pre-formed nuclei excited by compression-decompression. Bubbles may then migrate to critical sites elsewhere, or stick at the birth site. Moreover, nuclei are even present in every day live, especially during heavy sport activity. They may grow locally to the point where they cause deformation of the tissue and nerve endings beyond the pain threshold. They may dissolve locally by gaseous diffusion to surrounding tissue or blood or they may be minimized or eliminated by the pulmonary filter of the lungs.

A basic property of a bubble is its surface tension  $\gamma$ , the same, which do insect, walk on a water surface. For the underlying physics the reader is directed to Appendix 1. In addition the ambient pressure and the pressure in the bubble are of importance. The Laplace equation, holding for a bubble in equilibrium with the surrounding liquid, relates three parameters:

$$\begin{aligned} P_{\text{bubble gases}} &= P_{\text{ST}} + P_{\text{amb}} \\ &= 2\gamma/r + P_{\text{gases dissolved}} \end{aligned} \quad (6)$$

$P_{\text{bubble gases}}$  is the sum of the partial pressures of the composing types of gas in the bubble and its force is outside directed.  $P_{\text{ST}}$  is the pressure due to  $\gamma$  and is working inwards as do  $P_{\text{amb}}$ ,  $r$  is the bubble radius and  $P_{\text{amb}}$  the ambient pressure. Since equilibrium is supposed  $P_{\text{amb}} = P_{\text{gases dissolved}}$ .

Any bubble exceeding a critical size  $r^{\text{min}}$  will grow and any bubble smaller than this size will collapse (see Appendix 1 how this is calculated). In a normal non-supersaturated situation,  $r^{\text{min}}$  approaches infinity. So any bubbles are not expected around after a while. There is no bubble to grow: all bubbles will shrink.

Spontaneous bubble formation in pure liquids is extremely unlikely and would require huge pressures (some 1000 bar). So, in pure water immense supersaturations is possible, before bubbles are created. If no initial bubbles would be present in the water making up the diver, a diver could easily dive to a kilometer depth and go to the surface without any problems. In practice, this is not the case. Bubbles form on modest decompression as shallow as 10 m.

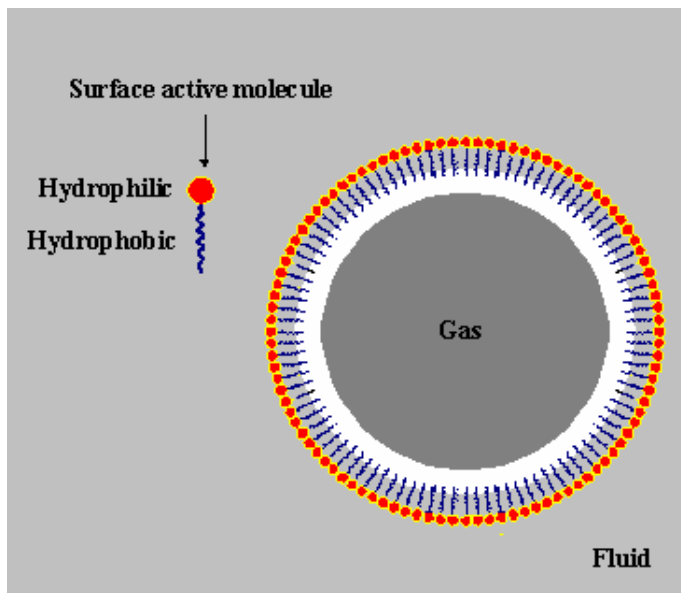


Fig. 9 The bubble skin comprised of surfactant molecules. (Modified after Reinders, 200x.)

The reason bubbles do form at relatively low pressures (a few bar) is due to nucleation, or bubble seeding on particles and surfaces in contact with the dissolved phase. Once formed, bubbles are then stabilized by the presence of surfactants, either already present

in blood and tissue, or released by tissue and vascular damage. The surfactant counteracts the effect of the surface tension.

The hydrophobic tails of the surfactant molecules (see Fig. 9) form a shield against the force of the surface tension of the water molecules and reduce the transport of gas molecules through the bubble skin. The underlying theory is described in Appendix 1.

### The Varying Permeability Model

Bubbles grow from micron size and although inherently unstable, they resist collapse due to elastic skins formed by surfactants or by a reduction in surface tension at tissue interfaces (see Fig. A1 in Appendix 1).

*The action of the surfactant is expressed in the equation:*

$$P_{\text{bubble gases}} + 2\gamma_c/r - B = P_{\text{amb}} + P_{\text{elast tissue}} + 2\gamma/r, \quad (7)$$

with  $P_{\text{surfactant}} = 2\gamma_c/r$ ,  $B$  the sum of electrical and chemical attractions and repulsions in the surfactant skin and to some extent the reservoir of surfactant directly surrounding the skin. Further,  $P_{\text{amb}} = P_{\text{hydrostatic}} = P_{\text{dissolved gases}}$ . This expression holds for equilibrium. When  $P_{\text{dissolved gases}}$  becomes smaller, for instance slowly by a controlled ascent, then the bubble shrinks since  $P_{\text{bubble gases}}$  is larger. However, first there is an initial grow due to the decreased hydrostatic pressure. When  $P_{\text{dissolved gases}}$  increases the bubble will grow.

In addition to the stabilising effect, the surfactant skin forms a barrier to diffusion. The

closer they are packed together, the stronger the barrier to diffusion

Once formed, very large pressures are needed to crush bubbles (tens of bars). This is one reason why saw-tooth like profiles or jo-jo's are bad, because the bubbles formed on each ascent phase are not crushed again at the descent. In fact, they accumulate, such that the final ascent and decompression phase is started with a pre-existing bubble load leading to a provocative situation. Since it is now recognized that the lifetime of a bubble can be measured in days or even a few weeks, this has implications for repetitive and multi-day diving, in particular. Bends often occur towards the end of multi-day dive trips, when bubble loads have been allowed to build up to a critical point.

Doppler detectable bubbles arise 1-2 hours after a (regular) dive in the blood. The question arises why the maximum Doppler signal occurs after about one hour and not for instance within 5 minutes after surfacing. This late Doppler response is not due to a too limited off-gassing capacity of the blood. Except for the first minutes, this capacity is always sufficient due to the halftime of blood of only about 60 seconds. During the ascent when the blood and the fast tissues are supersaturated many nuclei have the chance to pass the  $r_{\text{min}}$  limit. So, they grow into microbubbles. During the first 5 minutes of the surface interval when the blood and all tissues are supersaturated these bubbles can grow further. But the far majority, probably many millions and more, is much too small to be detected. After some 8 min after surfacing the blood is equilibrated with the ambient gas pressure. From now the microbubbles and silent bubbles (and the few detectable bubbles that did already arise) will not grow any longer. They will start shrinking. However, in massive amount they still circulate around. It is hypothesized that they have a large change to collide one another. In massive amounts they will coalesce. So, the Doppler bubbles arise since there is enough time for growing by fusion into real bubbles. The strength of the Doppler signal (numbers of bubbles and sizes) varies considerably among

subjects (also age, sex, condition, and BMI-matched subjects). Blood characteristics, which influence bubble stabilizing, so surfactant related factors, are supposed to play an important role. And these factors are supposed to be highly variable over the subjects.

Obviously, one way to reduce bubble loads for repetitive dives is to increase the surface interval between dives. It has been suggested that whilst it takes about 48 hours to achieve complete desaturation, it takes about 4 to 8 hours to get rid of most of the bubbles. Thus increasing surface time between dives to between 4 to 8 hours could decrease the risk of an event. Obviously these are complex processes, which escape complete elucidation. What is clear is that both free and dissolved gas phases must be taken into account in order to evolve safer and better decompression models. This is discussed in more detail in Appendix 1.

### Equilibrium:

External Pressure = Internal Pressure

$$P_{\text{AMBIENT}} + P_{\text{ST}} + P_{\text{ELASTIC}} = P_{\text{N}_2} + P_{\text{H}_2\text{O}} + P_{\text{CO}_2} + P_{\text{O}_2} + P_{\text{SURFACTANT}}$$

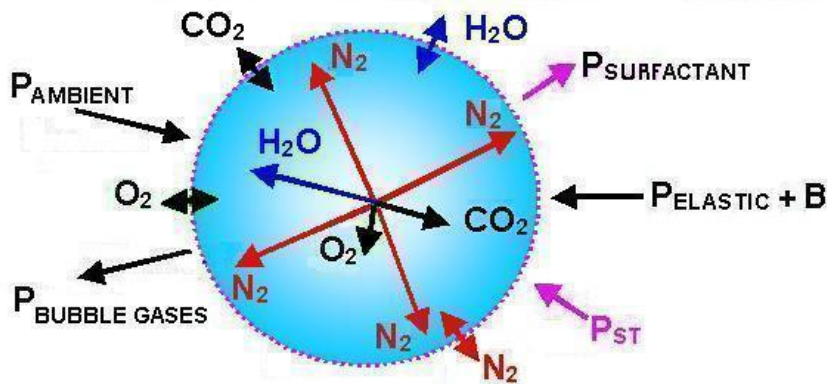


Fig. 10 External and internal pressures in equilibrium as described by the VPM model. Single headed arrows outside the bubble are pressures and their length is arbitrarily. The single headed arrows within the bubble denote the gas pressures of the four gases inside the bubble. The length of these arrows is in proportion to each other. For  $\text{N}_2$  one has to add the length of all 4 red arrows. The double-headed arrow visualizes the transport of gas molecules through the bubble skin. For a further explanation see Appendix 1. (Modified after Maiken, 1995.)

In what respects do VPM and RGBM differ?

RGBM has as a basis the Bühlmann model. It also includes the classical VPM bubble theory and from a practical point of view, after incorporating some extra modeling, RGBM DCs like Vyper and Cobra have the following features:

- For dives deeper than 30 m there is a reduction of the allowed bubble diffusion gradients within 2 hour time spans. This gives rise to the deep stop. In the ZH-L8 ADT model, also deep stops (more than one) are included (the 'microbubble-modes') but in that model total deco-time is substantially lengthened. This will increase the total nitrogen load of many tissues and slow down off-gassing of the faster tissues. In contrast, RGBM does not lengthen total deco-time. Two deep stops beyond 3 m are generally OK, also for most deco-dives.

- Restricted yo-yo and sharp bounce dives based on excitation of new nuclei.
- Restricted deeper-than-previous dives (reversed order) based on excitation of small nuclei over 2 hour time spans.
- Restricted multi-day diving based on adaptation and re-growth of new nuclei (also in recent versions of VPM).
- Consistent treatment of altitude diving, with proper zero-point extrapolation of limiting tensions and permissible bubble gradients (also in recent versions of VPM).

On the basis of the results of (Doppler) bubble and microbubble experiments the algorithm was further refined.

### New developments

The reality is that truly accurate decompression tables or computers will never be obtained. The complex nature of the physiology means that a certain amount of conservatism will be required. The best that can generally be hoped for are models that work most of the time. It is highly likely that current tables are much too conservative for some individuals, while being overly liberal for others. But for most people they will work rather well. As knowledge of decompression physiology improves, this holds out the hope of tables, or more likely DCs, tailored to some extent for the individual. An approach is to estimate the 'bubble load' based on personal biometrical data and the planned dive profile. Then the no-stop times can be adjusted to ensure a safe dive for that diver. An initial theoretical attempt along this line has recently been done by the author (Schellart, 2005).

## References

- Bühlmann A.A., von Völm E. Tachmedizin Barotrauma Gasenbolie Dekompression Dekompressionskrankheit, 3 auflage, 1993, Springer-Verlag, Heidelberg.
- Bühlmann A.A. Diving at altitude and flying after diving. In: The physiological basis of decompression, Vann R.D. (ed.) UHMS Workshop, 411-432, Bethesda, 1989.
- Chapman P. An explanation Professor A A Buhlmann's ZH-L16 Algorithm.  
[www.vvw.be/duiken/zhl16.doc](http://www.vvw.be/duiken/zhl16.doc), 200x
- Heads R. The trouble with bubbles,  
[http://www.kcl.ac.uk/depsta/biomedical/physiology/jp390/Diving\\_article.pdf](http://www.kcl.ac.uk/depsta/biomedical/physiology/jp390/Diving_article.pdf), 200x
- Reinders D. The Varying Permeability Model <ftp://decompression.org/pub/Reinders>, 200x.
- Maiken E. Bubble Decompression Strategies PART I: Background and theory, 1995.  
[www.decompression.org/maiken/Bubble\\_Decompression\\_Strategies.htm](http://www.decompression.org/maiken/Bubble_Decompression_Strategies.htm).
- Maiken E. VPMechanics 1-10.  
<http://www.decompression.org/maiken/VPM/RDPW/VPMech1/VPMech1.htm>. 1999-2001.
- Schellart NAM. Physics of compression chambers and medical physics of hyperbaric environments. A comprehensive treatise of well known and under-exposed effects, NVD Bulletin, 2002, 1-57. (Downloadable from [www.duikgeneeskunde.nl](http://www.duikgeneeskunde.nl)).
- Schellart NAM. Achtergronden van een theoretisch model over het risico op decompressieziekte met leeftijd, geslacht,  $VO_{2max}$  en lichaamsvetpercentage als parameters Is een correctie van de nultijd mogelijk? Met speciale aandacht voor vet% en  $VO_{2max}$ , 2005, [www.duikgeneeskunde.nl](http://www.duikgeneeskunde.nl), literatuur.
- Van de Velde. DeepOceanDiving's Diving Science, Decompression theory - neo-Haldane models, <http://www.deepocean.net/deepocean/index.php> van, 200x-2005.
- Wienke B.R., Reduced gradient bubble model, Best Publishing Co., Flagstaff, 2003.

## Abbreviations and symbols

a	subscript indicating arterial
<b>a</b>	compartment dependent constant in $P_{amb,tol}$ (bar absolute)
amb	subscript indicating ambient
<b>b</b>	compartment dependent direction coefficient in $P_{amb,tol}$ (dimensionless)
B	sum of electrical and chemical attractions and repulsions
d	depth, is $(P_{amb}-1)/10$ (pressure in msw)
DC	dive computer
$\Delta M$	= $1/b$ (dimensionless)
i	subscript indicating the inert fraction of a gas
ins	subscript indicating the inspired gas
$M_0$	= $10(a+1/b)$ (absolute pressure in msw)
M-value	= $M_0 + 10P_{compmax,i}$ (absolute pressure in msw), maximal tolerable inert gas pressure
n	subscript indicating number of compartment
$P_{amb,tol}$	maximal allowable ceiling of ascent (bar, absolute)
$P_{comp,i,begin}$	Inert gas pressure in the <i>compartment</i> at the <i>begin</i> of exposure (bar)
$P_{comp,i}$	Inert gas pressure in a compartment (bar)
$P_{comp,i}(t)$	the same but as a function of the exposure time $t$ (bar)
$P_{gases\ dissolved}$	total gas pressure in compartment
$P_{igas,ins}$	Inert <i>gas</i> pressure in the mixture being <i>inspired</i> (bar)
$P_{ss}^{min}$	= $(P_{tissue}-P_{amb})^{max}$ , the maximal allowable supersaturation gradient to prevent bubble growing with an initial radius larger than $r_0^{min}$ grow. The same for all compartments..
$P_{ss}^{new}$	New maximum allowed supersaturation gradient replacing $P_{ss}^{min}$ , resulting in a larger supersaturations and shorter deco times. Dependent on the halftime of the compartment and $t_D$ .
$P_{ST}$	pressure due to $\gamma$ (Pascal or bar)
$P_{stop}$	absolute ambient pressure at stop depth (bar)
r	bubble radius (m)
$r^{min}$	critical radius beyond which the bubble will grow
t	length of the exposure time (min)
$t_D$	total surfacing time
$T_{half}$	halftime (min)
$\tau$	time constant (min)
$\gamma$	surface tension (Newton/m or Pascal.m),
$\Gamma$	actual surface tension of surfactant skin; $0 < \Gamma < \gamma_c$ (Newton/m)
$\gamma_c$	maximal surface tension of surfactant skin (Newton/m),
v	subscript indicating venous
%M-value	percentual fraction of M-value reached by $P_{comp,i}$

## Appendix 1

### A deeper dive into VPM and RGBM

#### Surface tension

In physics, surface tension is an effect within the surface layer of a liquid (gas-liquid interface) that causes this layer to behave as an elastic sheet. It is the effect that allows insects (such as the water strider) to walk on water, and that causes capillary action. Surface tension is caused by the attraction between the liquid molecules, due to various intermolecular forces. In the bulk of the liquid, each molecule is pulled equally in all directions by neighboring liquid molecules, resulting in a net force of zero. At the surface of the liquid, the molecules are pulled inwards into the liquid by other molecules, but there are no liquid molecules on the outside to balance these forces. So, the surface molecules are subject to an inward force of molecular attraction, which is balanced by the resistance of the liquid to compression. There may also be a small outward attraction caused by air molecules, but as air is much less dense than the liquid, this force is negligible. Surface tension  $\gamma$  is measured in Newton's per meter ( $\text{N}\cdot\text{m}^{-1}$ ), and is defined as the force along a line of unit length perpendicular to the surface, or work done per unit area ( $\text{J}\cdot\text{m}^{-2}$ ). This means that surface tension can also be considered as surface energy, i.e. pressure (denoted as  $P_{\text{ST}}$ ). If a surface with surface pressure  $P_{\text{ST}}$  is expanded by a unit area, then the increase in the surface's stored energy is also equal to  $P_{\text{ST}}$ .

#### Gas bubbles in liquid

With a totally flat-water surface there is no force, which tries to pull a liquid molecule outside the liquid, provided that the gas above the surface is saturated with the molecules of the liquid. Systems try to minimize their (potential) energy, so the surface should be minimized. So, with a gas bubble in a liquid, the surface tension attempts to minimize the bubble's surface. Consequently, the surface tension is directed toward the center of the bubble. Hence, a bubble tends to shrink. However, then its volume decreases and this will increase the gas pressure in the bubble (Boyle's law), until equilibrium is established: so, the internal pressure compensates the sum of surface tension and ambient pressure. Shrinking does not happen when the bubble pressure  $P_{\text{bubble}}$  balances the surface tension  $\gamma$  plus the ambient pressure  $P_{\text{amb}}$ . The relation between the internal pressure due to the ambient pressure and surface tension is given by the Laplace equation:

$$P_{\text{bubble gases}} = P_{\text{ST}} + P_{\text{amb}} = 2\gamma/r + P_{\text{amb}}, \quad (\text{A1})$$

with  $r$  the radius.  $P_{\text{bubble gases}}$  is the sum of the partial pressures of the composing types of gas in the bubble. To do a calculation, pressures are expressed in Pa ( $= 1 \text{ N/m}^2 = 10^{-5} \text{ bar}$ ),  $r$  in m and  $\gamma$  in  $\text{J/m}^2$  or  $\text{N/m}$  (at  $0^\circ\text{C}$ ,  $\gamma$  of  $\text{N}_2$  in water is  $0.073 \text{ N/m}$ ).

The equation shows that smaller bubbles have higher pressures inside. The bubble principles apply to a balloon when trying to blow up. To get the first blow of air into the balloon (small radius) is hard, whereas it becomes easier if the balloon becomes larger.

#### Bubbles and diffusion

With a bottle of soft drink, things get more complicated. Bubbles in a soft drink and such-like, contain  $\text{CO}_2$ , as do the liquid itself.  $\text{CO}_2$  can diffuse from the solution into the bubble

or vice versa, depending on the  $PCO_2$  in solution and in the bubble. Assuming that the bubble consists of only  $CO_2$ , the  $PCO_2$  in the bubble is given by equation (A1) and depends on the radius. If the bottle is closed,  $PCO_2$  is in equilibrium with the ambient pressure  $P_{amb}$ . If it is assumed that there is only  $CO_2$  gas the (closed) bottle and that the liquid is saturated with  $CO_2$ . Then  $PCO_2$  will be equal to  $P_{amb}$  (neglecting hydrostatic pressure). The pressure in the bubble  $P_{in}$  will be higher than  $PCO_2$  outside due to the surface tension. Gas from within the bubble will diffuse into solution and the bubble will collapse. So every bubble will collapse due to this gradient  $P_{bubble\ CO_2} - P_{dissolved\ CO_2}$ . This is why in a closed bottle of a soft drink or beer there are no visible bubbles and there is no foam. However, if the bottle is opened things become different. The  $P_{amb}$  will drop suddenly, whereas the value of  $PCO_2$  in the liquid remains the same, at least for the moment. In this case  $PCO_2$  is larger than  $P_{amb}$ : the liquid is supersaturated with  $CO_2$ . Given  $P_{amb}$  and  $PCO_2$  in solution, there is a critical bubble radius  $r^{min}$  at which the pressure inside the bubble  $P_{bubble\ CO_2}$  equals  $PCO_2$ . The critical radius can be found by taking  $P_{bubble\ CO_2}$  in stead of  $P_{bubble\ gases}$  in equation (A1):

$$r^{min} = 2\gamma / (P_{water\ CO_2} - P_{amb}). \quad (A2)$$

For bubbles which size exceeds this critical size, the pressure  $P_{bubble\ gases}$  in the bubble is smaller than  $PCO_2$  in solution.  $CO_2$  will diffuse from the solution into the bubble. The bubble will grow. For bubbles smaller than the critical size, the opposite holds: gas from the bubble diffuses into solution and the bubble shrinks until it collapses completely. Bubbles at the critical size are in equilibrium, though it is an unstable equilibrium. So, every bubble with a radius larger than  $r^{min}$  will start to grow. In the opened bottle of soft drink bubbles becoming visible. Before opening there are also bubbles<sup>7</sup>, but they are too small ( $< 1\ \mu m$ ) to be visible. Due to opening the hydrostatic pressure in the bottle diminishes to 1 bar, so all bubbles expand according to Boyles law. Consequently, their pressure also becomes 1 bar. But after Boyle expansion they are still too small to be visible individually, but many are larger than  $r_{min}$ . They are heading for the surface while growing and more and more bubbles become visible. Their diameter might have doubled, tripled or more when they arrive at the surface. Of course, this growing during ascent has not to do with Boyle's law, since the differences in hydrostatic pressure in the bottle are nil. The growth of the bubble is due to a fast diffusion described above due to the large supersaturation of the liquid.

As an example, the critical radii for Spa Barisart Soda (6.4-8.0 g/l  $CO_2$ ) can be calculated. The pressure in the bottle specified by Spa is shown in next table (dependant on temperature). The  $PCO_2$  in solution is roughly that value. When opening the bottle the ambient pressure  $P_{amb}$  drops to 1 bar, whereas the partial pressure  $PCO_2$  remains at the high value. Using equation (A2) the critical radius  $r^{min}$  can be calculated.

The table was calculated with a  $P_{amb}$  of 1 bar (we open the bottle at atmospheric pressure). However would we have opened the bottle at a higher  $P_{amb}$ , then  $r^{min}$  is larger. For an ascending diver this means that the shallower the stop depth, the smaller  $r^{min}$ . Consequently more bubbles will exceed  $r^{min}$  and so more bubbles will grow.

---

<sup>7</sup> There are always gas nuclei formed at tiny irregularities of the wall and very small 'polluting' particles. The next section will deal with the stabilization of these nuclei.

Table 1A  $r^{\min}$  calculated with given  $P_{\text{water CO}_2}$  and ambient pressure 1 bar

Temperature (°C)	Pressure (bar= $10^5$ Pa)	$r^{\min}$ ( $\mu\text{m}$ )
15	3	0.73
20	3.75	0.53
25	4.5	0.42
30	5.3	0.34
35	6	0.29
40	7	0.24

### The surfactant as bubble stabilizer

The above equation (A1) holds for a pure liquid like water.

In a supersaturated situation any bubble exceeding a critical size  $r^{\min}$  will grow and any bubble smaller than this size will collapse. In a normal non-supersaturated situation,  $r^{\min}$  approaches infinity. As told before, any bubbles are not expected around after a while. To study bubble formation experiments have been done in gelatin. The advantage of gelatin over water is that any bubble appearing during decompression gets trapped and won't flow to the surface. In this way they can be observed and counted under a microscope. After decompression from a saturated condition, bubbles are formed in the sample. Pressure changes are so fast that in the first moments no gas is taken up or removed from any bubble.

In organic aqueous solutions and gelatin stable gaseous cavities are present, the nuclei with radii ranging from some 0.01  $\mu\text{m}$  up to around 1  $\mu\text{m}$ . Any nucleus in the solution larger than this will flow to the surface and disappear. Whereas in pure water an ordinary bubble with these radii would collapse under normal conditions (no supersaturation), these nuclei appear to be exceptionally stable and have a long life in a biological tissue.

Here comes in the *Varying Permeability Model (VPM)*. The VPM was initially defined by Yount c.s. and before him by Hill in order to give a quantitative explanation on the formation of bubbles in decompressed gelatin (as model for tissue).

According to the VPM, in biological systems there are generally molecules with a hydrophobic and hydrophilic part, like fatty acids. These molecules are surface active and form a monomolecular membrane at the interface with the hydrophobic end inside the gas and the hydrophilic end in the water (see Fig. 9 of main text). Yount proposed that this layer acts as an elastic skin, which account for the stability of the bubble. These molecules are the surfactant. The surfactant is of crucial importance to stabilize a bubble or for instance to maintain the shape of an alveolus. Without surfactant they will shrink immediately. Fig. 10 of the main text visualizes all the inside directed (i.e. acting on the bubble) and outside directed pressures when there is equilibrium described by the VPM model. The figure also visualizes the transport of gas molecules through the bubble skin (double headed arrow) and the contribution by the four types of gas in the inside pressure, the arrows inside the bubble. They denote the partial gas pressures and their length is proportional to that pressures. Remarkably is the very small arrow of  $\text{PO}_2$ . Indeed in active tissue, e.g. brain muscle tissue it is smaller than that of  $\text{CO}_2$  and  $\text{H}_2\text{O}$ . When there is complete saturation, the sum of the four partial pressures is considerably smaller than that of the pressure of the inspired air and even of that of the alveoli. The deficit is caused by the ongoing consumption of oxygen: the oxygen window that has been discussed before. During the compression stage, these skins are permeable for gas up to a pressure of around 9 bar.

Just as the water molecules at the interface “pull” towards each other in surface tension, the surface-active molecules “push” against each other. So, the force is directed outward. This counteracts the effect of surface tension, and therefore eliminates the loss of gas in the bubble by diffusion. This membrane reduces the motion of gas molecules from the bubble to the liquid and vice versa.  $P_{\text{surfactant}}$  is:

$$P_{\text{surfactant}} = 2\Gamma/r \quad (\text{A3})$$

$\Gamma$  accounts for the springy “push back” effect of the surfactants. It varies:  $0 < \Gamma < \gamma_c$ , which makes the Permeability Model *Variable* (VPM), as does the permeability limit at about 9 bar. The actual value of  $\Gamma$  depends on the degree of tightness of the packing of the surfactant monolayer. When the packing becomes too loose, new surfactant molecules can be recruited from a reservoir, which wraps the monolayer.  $\gamma_c$  is 0.257 N/m, about 14 times  $\gamma$ . So, the stabilizing effect can be enormous. In addition to the effect of the surfactant there are also various electrical and chemical attractions and repulsions.  $B$  denotes their sum. In the surrounding tissue there is another force, which tries to crush the bubble caused by the elasticity of the tissue. Finally, when everything is in equilibrium, equation (A1) becomes:

$$P_{\text{bubble gases}} + 2\Gamma/r - B = P_{\text{dissolved gases}} + P_{\text{elast tissue}} + 2\gamma/r, \quad (\text{A4a})$$

with  $P_{\text{dissolved gases}} = P_{\text{amb}} = P_{\text{hydrostatic}}$ . (Some authors include  $P_{\text{elast tissue}}$  in  $P_{\text{amb}}$ .)

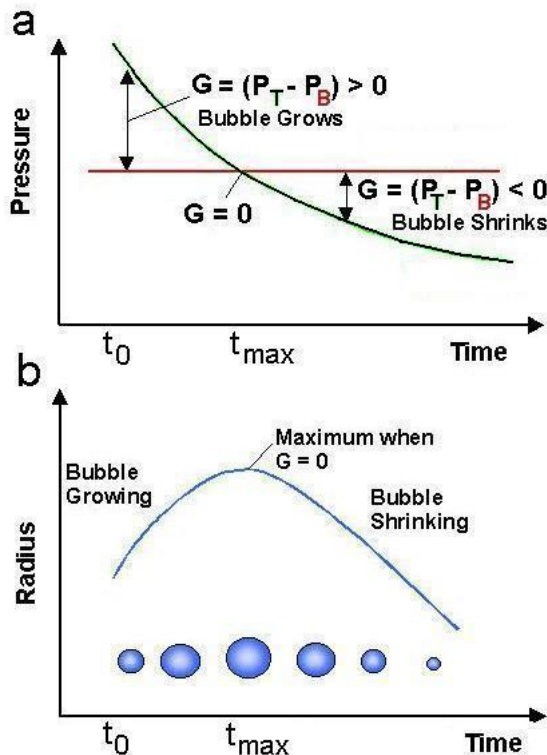


Fig. A1  $P_{\text{tissue}}$  ( $P_T$ ) and  $P_{\text{bubble}}$  ( $P_B$ ) as function of time (a) and bubble radius versus time (b). At  $t=t_0$ ,  $P_{\text{tissue}} > P_{\text{bubble}}$ . Now,  $P_{\text{tissue}}$  is slowly diminished and the bubble will grow due arising supersaturation of the tissue. At  $t=t_{\text{max}}$ , an unstable new equilibrium is reached and a further decrease of  $P_{\text{tissue}}$  makes the bubble to shrink. (Modified after Maiken, 1995.)

Notice that (A4a) is independent of the compartment characteristics (halftime, **a** and **b**). Suppose that  $r=1 \mu\text{m}$  and  $P_{\text{amb}} = 4 \text{ bar}$  (about 30 msw), than with the maximum value of  $\Gamma$ , the pressure caused by the surfactant is about 5 bar. In equilibrium with moderate values of  $\Gamma$ , taking also  $B$  into account,  $P_{\text{bubble gases}}$  will be about 1-2 bar less than  $P_{\text{dissolved gases}}$ .

### From equilibrium to in- and outflow

The short notation of equation can (A4a) is  $P_{\text{bubble}} = P_{\text{tissue}}$ . A change of  $P_{\text{tissue}}$  will be caused by a change in  $P_{\text{amb}}$ , since the other terms are constant. The difference between  $P_{\text{tissue}}$  and  $P_{\text{bubble}}$  is called the gradient  $G$ :

$$G = P_{\text{tissue}} - P_{\text{bubble}} \quad (\text{A4b})$$

(Various authors restrict the two  $P$ 's of (A4b) to the inert gases or nitrogen, as is the case in the next two figures). As soon as  $P_{\text{tissue}} \neq P_{\text{bubble}}$ , due to compression or decompression (change of  $P_{\text{hydrostatic}}$ ), the equilibrium can be restored by gas transport through the bubble skin. In (A4a)  $P_{\text{bubble gases}}$  should now be replaced by  $P_{\text{hydrostatic}}$ . According to Boyle's law  $r$  will change (but less than the law).  $\Gamma$  and  $B$  also change due to the smaller or larger diameter, which yields another packing. With a small change, the number of molecules in the skin does not change and there is no gas transport. With a large compression molecules can be squeezed out of the skin and with a large decompression molecules are taken up. This all makes that the total change of  $r$  and the gas transport cannot be calculated precisely. Anyway, with decompression  $r$  becomes larger due to the diminished hydrostatic pressure, but only a large change evokes gas transport. Above a critical  $r$ ,  $r_0^{\text{min}}$ , a microbubble will grow into a real bubble. However, beyond this limit first the microbubble grows and when its radius stays beyond the critical limit, the microbubble will finally start shrinking. This shrinking is caused by off-gassing of the tissue, and dependent on  $T_{\text{half}}$ , starts within some (tens of) minutes (Fig. A2b).

*With a strong and fast compression to a new  $P_{\text{amb}}$ , a microbubble can be crushed according to (Reinders, 200x):*

$$\begin{aligned} r_{\text{crush}} &= 1/(0.5(P_{\text{amb}} - P_{\text{tissue}})/(\Gamma - \gamma) + 1/r_0) \\ &= r_0/(0.5r_0(P_{\text{amb}} - P_{\text{tissue}})/(\Gamma - \gamma) + 1) \end{aligned} \quad (\text{A5})$$

*with  $r_0$  the original radius.  $r_{\text{crush}}$  is of interest for a wet or a surface decompression. An example shows what happens. For  $r_0 = 1 \mu\text{m}$  (often used in the bubble literature),  $\Gamma = \gamma_C$  and  $(P_{\text{amb}} - P_{\text{tissue}}) = 1 \text{ bar}$  and  $r_{\text{crush}}$  becomes about  $0.9 \mu\text{m}$ . This is a small decrease in size (even smaller with  $\Gamma < \gamma_C$ ) and one can doubt about its relevance. Surprising is that the pressure difference in the equation is of importance and not the pressure ratio (as in Boyle's law). The crushing model is experimentally used to examine whether the bubble load decreases when after the safety stop a short stop is made at about 9 m and then surface.*

Resuming: with a negative  $G$  (slow ascent) the bubble will release inert gas to restore equilibrium and with a positive  $G$  the bubble will grow (so a negative  $G$  means negative grow or shrinking). Both processes are illustrated in Fig. A1.

The liquid models dictate a stop depth as shallow as possible to accelerate off-gassing. This is visualized in the upper panel of Fig. A2. The bubble models dictate a slow ascent to enable shrinking and an ascent to a deeper stop-depth to limit  $G$  and consequently the

volume of the gas transport. This is illustrated in the lower panel of Fig. A2. This panel is the conceptual backbone of the bubble models: at any time  $P_{\text{comp},i}$  and  $P_{\text{bubble},i}$  are calculated and compared to see what happens. However, gas transport through the skin, although fast, needs time. When the ascent is too vast ( $> 10$  m/min) there is not time enough for the bubble to release gas. Due to the 'explosive' ascent the bubble will expand as was described for the Spa bottle.

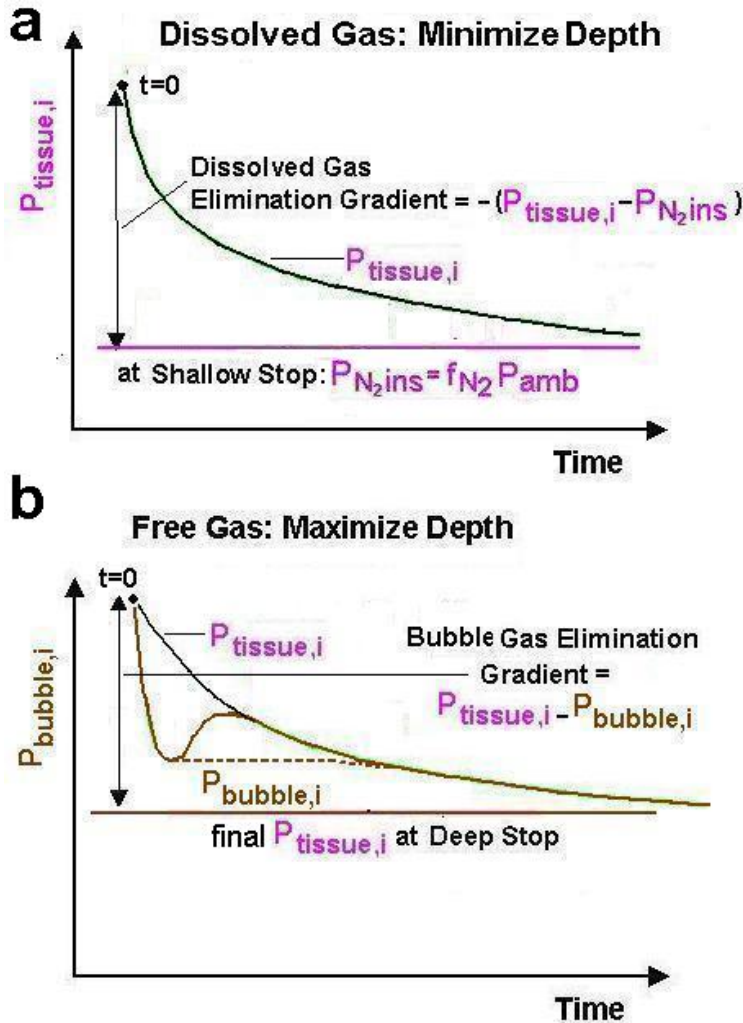


Fig. A2 a.  $P_{\text{bubble},i}$  as a function of time according to a Neo-Haldanian model when an ascent is made to a stop depth.  $f_{N_2} = 0.79$ . b. The fast initial decrease of  $P_{\text{bubble},i}$  is due to a Boyle like behavior and subsequent small grow and small increase of  $P_{\text{bubble},i}$  is dependent on the bubble size at the stop depth. With a small gradient there is no increase. Its time course is rather arbitrarily drawn. Actually, not  $P_{N_2,ins}$  but  $P_{N_2,alveolar}$  is relevant for the dissolved gas elimination. See the text for a further explanation. (The original basis of this figure comes from Maiken, 1995.)

An example will illustrate what happens more precisely when the ascent is not too large and too fast. Suppose that an ascent is made from 40 to 15 meter, and that at 40 m the tissue and bubble  $P_{N_2}$  (in equilibrium with compartment) was  $4 \times 0.79$  bar (so compartment sub-saturated). Due to the ascent, the (micro/silent) bubble will double in volume (a diameter increase of 26%) and half in pressure when Boyle's law holds. Then, at 15 m, its

$P_{\text{bubble},i}$  is  $2.5 \times 0.79 = 1.98$  bar. With an infinite fast ascent, the inert gas pressure difference between the tissue and the bubble after arriving is  $(4-2.5) \times 0.79$  bar. However, the ascent lasts 2.5 min. With a 2.5 min compartment (the fastest compartment of RGBM) half its supersaturated part of  $P_{N_2}$  is eliminated at arrival. So,  $P_{\text{comp},i,15\text{m}}$  is  $(2.5+0.5 \times (4-2.5)) \times 0.79 = 2.56$  bar. So, the difference between  $P_{\text{comp},i,15\text{m}}$  and  $P_{\text{bubble},i}$  at arrival, the gradient  $G$ , is  $+0.58$  bar. The ascent rate was correct and 15 m can be considered as a deep stop. Yet, the outcome suggests that the bubble will grow and not shrink! What happens?

When the diameter increase is small the packing in the skin remains tight enough in order to prevent recruitment of new surfactant molecules from the reservoir. Bubble can resist a reasonable amount of supersaturation in the tissue without gas uptake since the surfactant molecules attract each other. This is also understandable from the M-value concept: when  $P_{\text{comp},i,15\text{m}}$  is close to or exceeds the M-value, the supersaturation causes massive growing and arising of (silent) bubbles. From Bühlmann's theory, at 15 m the M-value for a hypothetical 2.5 min compartment is even 8.2 bar. Going back to the example, the difference of 0.58 bar is really small.

Summarizing: with a regular ascent rate, the Boyle expansion in the fastest compartments is never reached since:

- 1) the supersaturated compartment is off-gassing during the ascent;
- 2) the coherent forces in surfactant skin hampers expansion;
- 3) the tight packing of surfactant molecules limits rapid gas transport.

The get an idea of a lower value of the increase of the bubble radius at the start of the stop it is supposed that already then there is an equilibrium of the inert gas pressures, so  $P_{\text{bubble},i} = P_{\text{comp},i}$ . The diameter increase appears to be 15.5% ( $=100(5/(2.56/0.79)^{1/3}-1)\%$ ) compared to 40 m. With a deep stop at 25 m, a much better choice, the increase in diameter is only 9.2% larger, a value that holds the packing possibly too tight to allow easy gas transport and to allow recruitment of new surfactant molecules. When the actual increase in radius is less, the bubble starts to eliminate inert gas from the beginning of the ascent. If not, elimination starts during the stop, at the moment that the actual  $P_{\text{bubble},i \text{ stop}}$  equals  $P_{\text{comp},i}(t)$  after some off-gassing of the compartment. This principle is indicated by the dashed horizontal line in Fig. A2b. In a worse case, some nitrogen can invade the bubble, and this is indicated by the solid line first going up, peaking and then going down, just as the exponential decrease of  $P_{\text{comp},i}(t)$ . In this case, the bubble expands a little. When the ascent is too large,  $r^{\text{min}}$  becomes too small and  $G$  becomes too large. New molecules have to be recruited from the surfactant reservoir directly surrounding the skin, since there are too few molecules to preserve the skin. This changes  $2 \Gamma/r - B$  of (A4a) and now the gas transport will happen inward to obtain a new equilibrium. The remedy is reducing the gradient: the reduced gradient concept of RGBM.

When the ascent is too fast, the skin cannot adapt fast enough to the new larger surface and has to reorganize by incorporating new surfactant molecules, just as with a too large ascent. Also now, the bubble will take up inert gas and this will not stop soon, since now much grow is possible.

In both cases growing continues until a new equilibrium is reached and a well-grown 'adult' bubble is the result.

How can the safety stop be interpreted with the knowledge of the behavior of dissolved and free gas? This stop is too short to attribute to off-gassing of all compartment except those with  $T_{\text{half}} < 12$  min. The fastest component has the highest M-value and is generally not at risk during the safety stop. So, the safety stop is not an off-gassing stop but predominantly an anti-bubble-grow stop. However, 3 m is rather shallow, 4.5 m (15 feet) is advised. Obligate stops are based on Haldanian and bubble theory.

The above is a simplification, of theory and the more for reality. Amongst others, the other gases and the oxygen window was not taken into account.

Recent bubble models are more refined. They calculate a maximum allowed supersaturation gradient is  $(P_{\text{tissue}} - P_{\text{amb}})^{\text{max}}$ . This is where nuclei with an initial radius (at the start of the dive) larger than  $r_0^{\text{min}}$  start at some time growing into a bubble. Any gradient smaller than this, called  $P_{\text{ss}}^{\text{min}}$  value will not result in grow, so this will result in less bubbles. To calculate  $P_{\text{ss}}^{\text{min}}$ , which is the same for all compartments, the various authors use slightly different equations. I adopted a version, which shows dependency on  $(P_{\text{deepest}} - P_{\text{surface}})$ , see VP Mechanics1 of Maiken (1999).

The gas transport through the skin is dependent on the rate of diffusion and indirect also on the perfusion of the tissue. In this way the, say 16, tissue halftimes come in. A new variable is defined for the maximal allowed supersaturation:  $P_{\text{ss}}^{\text{new}}$ . It replaces  $P_{\text{ss}}^{\text{min}}$ , but is different for all compartments and is related with total surfacing time  $t_D$ .  $P_{\text{ss}}^{\text{new}}$  results in a larger permitted supersaturations and shorter deco times. The derivation of  $P_{\text{ss}}^{\text{new}}$  is treated by van der Velde and can also be found in one of Younts papers. Although it comprises six assumptions, seen from diving practice (DCS risk) the outcomes appear to be useful and reliable. The derivation takes into account a fixed  $r^{\text{min}}$  and fixed safe number of bubbles, and as variables the actual number of bubbles with their size distribution, and the supersaturation gradient  $(P_{\text{tissue}}(t) - P_{\text{amb}}(t))$ , and this for all compartments. Finally, a critical total bubble volume  $V_{\text{crit}}$  is chosen. For a given deco-profile and a starting value of  $t_D$  the above variables are calculated. The strategy is to let  $t_D$  and the whole set of  $P_{\text{ss}}^{\text{new}}$  converging. After each iteration a new critical bubble radius,  $r_0^{\text{new}}$  results. This is, seemingly paradoxically, smaller than  $r_0^{\text{min}}$ . Also  $t_D$  becomes smaller and the G values (as function of time) become larger, they are maximized. The  $P_{\text{ss}}^{\text{new}}$  values are larger than  $P_{\text{ss}}^{\text{min}}$ , the more the faster the compartment. In the faster compartments after ascent, part of the bubbles can grow but their total volume does not exceed  $V_{\text{crit}}$ .

The finally found values of  $P_{\text{ss}}^{\text{new}}$  are now applied as M-values, just as in the liquid models. The slowest compartments have slightly higher M-values for all depths than the Bühlmann ZH-L16 M-values. The fastest compartments have smaller ones at depths larger than about 15 m, which makes RGBM and VPM more conservative for deep dives and consequently the deep stop attractive. For smaller depths all the compartments have larger M-values, which increase zero times and shorten stop times. Recent refinements include altitude diving with parameter depth dependent parameters. This resulted in curved M-value lines, which converge at zero at zero ambient pressure.